TRANSPORTATION RESEARCH RECORD 645

Bridge Tests

TRANSPORTATION RESEARCH BOARD

COMMISSION ON SOCIOTECHNICAL SYSTEMS
NATIONAL RESEARCH COUNCIL

NATIONAL ACADEMY OF SCIENCES
WASHINGTON, D.C. 1977

Transportation Research Record 645
Price $3.00
Edited for TRB by Mary McLaughlin

subject areas
27 bridge design
33 construction

Transportation Research Board publications are available by ordering directly from the board. They may also be obtained on a regular basis through organizational or individual supporting membership in the board; members or library subscribers are eligible for substantial discounts. For further information, write to the Transportation Research Board, National Academy of Sciences, 2101 Constitution Avenue, N.W., Washington, D.C. 20418.

Notice

The project that is the subject of this report was approved by the Governing Board of the National Research Council, whose members are drawn from the councils of the National Academy of Sciences, the National Academy of Engineering, and the Institute of Medicine. The members of the committee responsible for the report were chosen for their special competence and with regard for appropriate balance.

This report has been reviewed by a group other than the authors according to procedures approved by a Report Review Committee consisting of members of the National Academy of Sciences, the National Academy of Engineering, and the Institute of Medicine.

The views expressed in this report are those of the authors and do not necessarily reflect the view of the committee, the Transportation Research Board, the National Academy of Sciences, or the sponsors of the project.

Library of Congress Cataloging in Publication Data
National Research Council. Transportation Research Board.
Bridge tests.

(Transportation research record; 645)
Includes bibliographical references.
1. Bridges–Testing–Addresses, essays, lectures. I. Title. II. Series.
TE7.H5 no. 645 [TG305] 380'.5'08s [624.2'028]
ISBN 0-309-02674-1 78-17950

Sponsorship of the Papers in This Transportation Research Record

GROUP 2–DESIGN AND CONSTRUCTION OF TRANSPORTATION FACILITIES
Eldon J. Yoder, Purdue University, chairman

Structures Section
Ivan M. Viest, Bethlehem Steel Corporation, chairman

Committee on Steel Bridges
John W. Fisher, Lehigh University, chairman
J. Hartley Daniels, Lehigh University, secretary
Dan S. Bechly, Russell L. Chapman, Jr., Lionel F. Currier, Arthur L. Elliott, Gerard F. Fox, Karl H. Frank, T. V. Galambos, Carl H. Gronquist, Wayne Henneberger, William A. Kline, Andrew Lally, Joseph M. McCabe, Jr., Roy L. Mion, Frank D. Sears, Michael M. Sprinkel, Ivan M. Viest, Charles H. Wilson

Committee on Concrete Bridges
Cornie L. Hulsbos, University of New Mexico, chairman
John M. Hanson, Wiss, Janey, Elstner and Associates, secretary
T. Alberdi, Jr., John F. Cavanaugh, W. Gene Corley, Hotten A. Elleby, Norris L. Hickerson, David S. Huval, Walter J. Jestings, Heinz P. Koretzky, H. G. Kriegel, George F. Leyh, Charles C. Mitchell, Joseph H. Moore, Emile G. Paulet, Dominick L. Somma, David A. Van Horn, Earle E. Wilkinson

Committee on Dynamics and Field Testing of Bridges
Conrad P. Heins, Jr., University of Maryland, chairman
Charles F. Galambos, Federal Highway Administration, secretary
James W. Baldwin, Jr., Edwin G. Burdette, William G. Byers, Paul F. Csagoly, Cornie L. Hulsbos, Henry L. Kinnier, Celal N. Kostem, Robert H. Lee, Kenneth H. Lenzen, Norman G. Marks, Fred Moses, M. Noyszewski, Leroy T. Dehler, Frederick H. Ray, Ronald R. Salmons, W. W. Sanders, Jr., Robert F. Varney, William H. Walker, George W. Zuurbier

Lawrence F. Spaine, Transportation Research Board staff

Sponsorship is indicated by a footnote at the end of each report. The organizational units and officers and members are as of December 31, 1976.

Contents

COMPOSITE BOX-GIRDER BRIDGES DURING CONSTRUCTION
Roger Green and David Strevel 1

EFFECTS OF DIAPHRAGMS ON LATERAL LOAD DISTRIBUTION IN BEAM-SLAB BRIDGES
Celal N. Kostem and Ernesto S. deCastro 6

SURVEY OF FIELD AND LABORATORY TESTS ON BRIDGE SYSTEMS
Hota V. S. GangaRao 10

HIGHWAY BRIDGE VIBRATION STUDIES
John T. Gaunt, Trakool Aramraks, Martin J. Gutzwiller, and Robert H. Lee 15

LOAD DISTRIBUTION ON A TIMBER-DECK AND STEEL-GIRDER BRIDGE (Abridgment)
Marvin H. Hilton and L. L. Ichter 20

DYNAMIC PROPERTIES OF BEAM-SLAB HIGHWAY BRIDGES (Abridgment)
Celal N. Kostem 23

PORTABLE RECORDER FOR BRIDGE STRESSES
Mark W. Williams and James W. Baldwin, Jr. 25

Composite Box-Girder Bridges During Construction

Roger Green and David Strevel, Department of Civil Engineering,
University of Waterloo

A 1/20 scale-model study of simple-span girders was undertaken to examine the effect of a typical construction loading on both single open-section and quasi-closed-section girders and interconnected girders. Deflections, distortion, and stresses resulting from the torsional loading on these girder systems were observed. The response of an open, simple-span girder, braced to minimize distortion, can be predicted with available theories for mixed torsion. A quasi-closed girder generally behaves as a closed section and St. Venant shear stresses resist applied torsional loadings. However, the quasi-closed girder was found to have only 40 percent of the theoretical torsional stiffness value. Studies of interconnected boxes with end diaphragms and simple tie bracing at the one-third span points indicate that simple tie bracing significantly reduces the torsional rotation of open sections. This bracing can remain in place without affecting the appearance of the girder system. Bracing is necessary to maintain the stability of open sections during construction. Considering symmetry can help to minimize torsional construction loads on individual girders. Geometrically and structurally stable configurations can be designed for construction loadings by using simple bracing schemes.

Composite steel-concrete box-girder bridges have been favored in many locations in North America for intermediate-span bridge structures since design procedures were outlined in the mid-1960s (1, 2). Since these design procedures were accepted, simple- and continuous-span structures with individual spans varying from 20 to 100 m have been used for river crossings and grade separations at urban intersections.

The completed structure, which is aesthetically pleasing, consists of steel box girders made composite with a concrete deck slab. Economies in design are possible because the completed box-girder section has a higher torsional stiffness and a greater lateral distribution of live load than an I-beam structure with similar flexural strength. Additional economies are also possible in the fabrication and erection of box girders, compared to similar I-beam structures, because of the elimination of much of the wind and transverse diaphragm bracing.

A number of cross-sectional geometries of the completed structure are possible; the number of girders can vary from two to six or more depending on the plan geometry of the structure. Three typical cross-sectional geometries for two-box-girder systems, with single and double bearing arrangements and shallow and deep end-support diaphragms, are shown in Figure 1. Typical spacing of the centerline of the box girders varies from 4.3 to 6.7 m, and the depth of the cast-in-place concrete deck varies from 190 to 250 mm. The ratio of dead-load moment to live-load moment for box-girder structures will thus depend on the cross section, the depth of the deck, and the span arrangement chosen by the design engineer.

Experience with the construction of box-girder systems has indicated that the design specifications of 1968 to 1973 (1, 2, 3) do not provide design or construction engineers with sufficient guidance regarding the behavior of thin-walled flexible box girders during construction. The specifications do not clearly identify the need for intermediate diaphragms or cross-frames that would retain the cross-sectional geometry of the girder during fabrication and handling. Structural steel fabricators have often added bracing within the girders, but calculation procedures allowing for the design of such bracing are not given in the specifications or the design criteria (1, 2). The responsibility for the bracing of girders during construction is frequently given to the general contractor, who normally does not have access to the structural design calculations. Designing construction bracing systems without referring to the original design calculations can be difficult.

The current Canadian specification (4) does refer to forces acting during the construction phase and indicates that diaphragms (bracing) shall be used to cater for flexural distortional and warping stresses. But selection of calculation procedures for the construction-phase loading is left to the designer. This situation can lead to the use of box girders with excessive bracing and thus result in waste of material and labor.

Many of the construction difficulties mentioned above appear to have arisen from a misapplication of research data on composite box-girder systems. The research data that support the current design specifications for the analysis and proportioning of box-girder systems (5) appear to apply only to the characteristics of live load distribution for straight bridge spans of up to about 45 m. Bridge models at one-quarter scale were considered in the studies, but there was no consideration of dead-load similitude. Thus, dead-load force effects in an equivalent prototype structure were not fully represented in the research nor in the subsequent specifications (1, 2, 3).

This paper describes the possible loading configurations present during construction on a thin-walled box-girder system and examines the resulting stresses induced in typical torsionally open and torsionally quasi-closed box girders. The stress analyses are based on the results of 1/20 scale-model tests supplemented by a mixed torsion analysis of individual open and quasi-closed box sections. A variety of bracing systems are discussed that will minimize the additional longitudinal stresses caused by torsion in open box-girder systems.

NOTATION

The following notation was used in this study of construction loading on box-girder bridges:

- b = average width of girder
- D = spacing of distortional bracing
- e = eccentricity of loading with respect to centerline of girder
- e_f = eccentricity caused by formwork
- e_p = eccentricity caused by finishing plant
- e_v = eccentricity caused by vertical load
- e_w = eccentricity caused by wind
- h = height of girder
- I_x = moment of inertia about x axis
- I_y = moment of inertia about y axis
- I_ω = sectorial moment of inertia
- l, L = span length
- m = distributed torsional moment
- m_c = moment caused by concrete
- m_f = moment caused by formwork
- m_v = moment caused by vertical load
- m_w = moment caused by wind
- W_c = weight of concrete per unit length

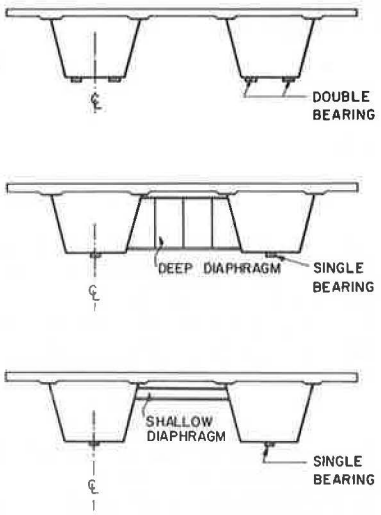

Figure 1. Typical cross-sectional geometries for three box-girder systems.

Figure 2. Loading as a result of concrete deck.

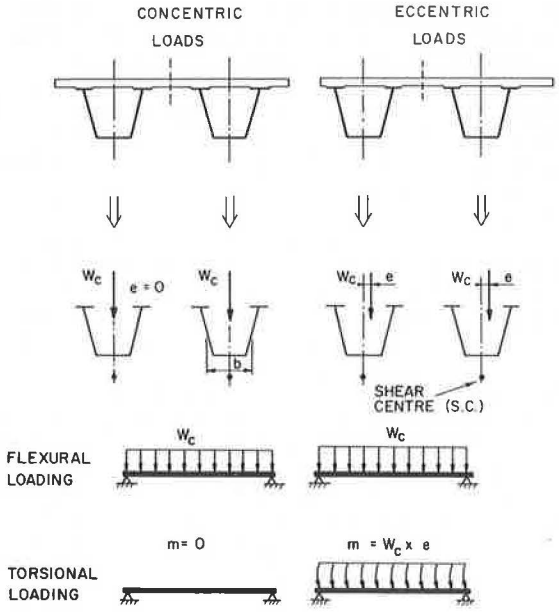

W_v = vertical load per unit length
W_w = wind load per unit length

CONSTRUCTION LOADINGS

As part of the design process the design engineer selects a sectional geometry and establishes the position of the concrete deck relative to the centerlines of the individual box girders and the complete box system. Two examples of cross-sectional arrangements are shown in Figure 2. In the concentric-loading case, the weight of the fresh concrete results in only flexural stresses. The compression flanges of each box girder require bracing to avoid the lateral buckling that results from the combined action of vertical load and the horizontal component of the force in the web.

As a result of geometric or other constraints, the designer may choose a cross-sectional geometry in which the deck concrete gives rise to eccentric loading of the individual girders in the simplified box-girder structure (Figure 2). This case gives rise to a uniformly distributed load (W_c) located at a transverse eccentricity (e) with respect to the centerline of individual box girders and results in both flexural and torsional loadings as shown in Figure 2.

The end reactions provide a restraint for shear caused by the vertical loading. Restraint for the torsional loading is also required and can easily be provided as part of the design of end-support systems 1 and 2 in Figure 1. The shallow diaphragm and single-support case (end-support system 3 in Figure 1) requires special design and detailing to ensure adequate strength and stiffness for torsional loading.

Other construction loadings that give rise to predictable torsional effects during design include wind loading of the exposed girders, the finishing machine, and the formwork. Additional torsional loadings result from the concrete-handling systems chosen by the general contractor and the unsymmetrical placing of deck concrete. These loadings can be minimized by careful specification.

Construction-stage loadings for a number of Canadian box-girder bridges were examined. Typical vertical loads resulting from concrete plus formwork were found to be between 25 and 40 kN/m, and the horizontal loads due to wind were found to be between 2 and 3.5 kN/m. These load types result in shear and bending moment diagrams that have forms familiar to designers. The flexural loads act eccentrically to the shear center and give rise to torsional loading. The ratio (e_v/b) of the eccentricity of the vertical loads from the centerline of the girder (e_v) to the average girder width (b) varies from 0 to 0.14 (the shear center lies on the axis of symmetry). The analysis of the typical box-girder sections indicates that the vertical and horizontal loads and associated torsional loads vary from structure to structure. The values of torsional loading are controlled by the design engineer's choice of cross-sectional geometry.

MODEL STUDIES

A series of scale-model tests of thin-walled members was initiated to develop a more complete understanding of the distortional and warping stresses that occur in eccentrically loaded box-girder systems during construction. These tests relate to the response to flexural and torsional loading of both single box girders and multiple interconnected box girders.

To establish the dimensions of the scale-model structures, the geometries of a series of prototype steel box-girder bridges provided by the Canadian Steel Industries Construction Council were examined; typical ratios obtained for base width to height, top width to height, and width to girder spacing are given in Table 1. In addition, ratios of width or height to thickness were also calculated for top and bottom flange plates and webs. These data were used to proportion a cross-sectional geometry representative of a typical structure with unstiffened webs (Figure 3). The cross-sectional geometry of the resulting model structure, scaled to $^1/_{20}$, is shown in Figure 4. To develop this geometry it was necessary to make minor adjustments to the results of the nondimensional study of prototype structures.

Figure 5 shows the two types of box girders that were developed by using the basic model geometry: (a) a torsionally open section that included distortional bracing to minimize possible cross-sectional distortion of the model under the action of torsional load and (b) a torsionally quasi-closed section, which was the result of including top chord bracing in the model. The distortional bracing was located at a spacing of three member depths for both types of box girders (Figure 6) and is representative of prototype structures (Table 1). The plan arrangement of the top chord bracing for the quasi-closed box girders is also shown in Figure 6. Rods were

Table 1. Typical prototype geometries of steel box-girder bridges.

Bridge	Type	Span 1 (m)	Span 2 (m)	Girder b (m)	Girder h (m)	Girder b/h (m)	e_v (mm)	e_v/b Ratio	Web Slope	D/h
a	C[a]	42.4	42.7	2.06	1.68	1.23	—	—	4.4/1	9.2
b	C[a]	64.0	77.7	2.67	2.90	0.92	172	0.064	4.2/1	2.7
c	S[b]	63.4	—	2.01	2.01	1.00	120	0.060	4.3/1	3.9
d	C[a]	59.4	76.2	2.29	2.44	0.94	122	0.044	5.3/1	3.1
e	S[b]	42.7	—	2.19	1.62	1.34	254	0.116	4.6/1	4.4
f	C[a]	44.5	56.4	2.40	2.26	1.06	229	0.095	2.4/1	5.0
g	C[a]	61.0	85.3	2.21	2.49	0.89	343	0.138	6.5/1	—

[a]Continuous-span system. [b]Simple-span system.

Figure 3. Cross section of typical prototype geometry derived from Table 1.

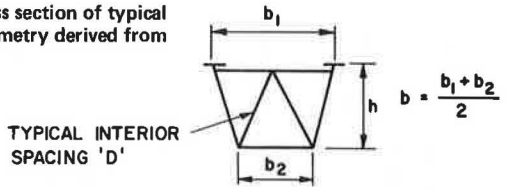

Figure 4. Cross-sectional geometry of prototype and model sections.

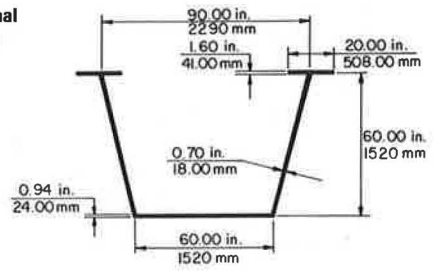

Figure 5. Open and quasi-closed members.

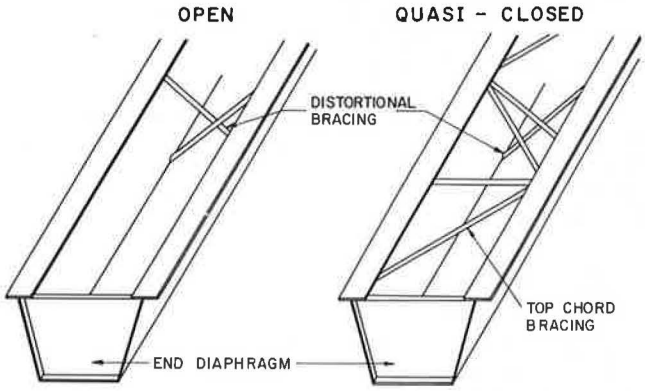

Figure 6. Plan of model girders.

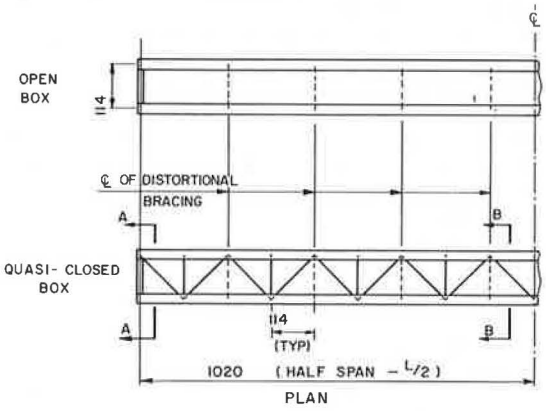

used throughout for the bracing members and were designed by using a maximum slenderness ratio of approximately 200. The models were carefully fabricated to minimize distortion and imperfections caused by welding. An aluminum jig was used to ensure that the desired geometry was maintained (6).

The models have a span length of 2030 mm and a total length of 2057 mm. The span-to-depth ratio of the simply supported system is approximately 27. The reaction system provided at each end of the models (Section A-A in Figure 7) consists of two load cells, a cross beam, and a solid end diaphragm that allows for transfer of shear forces from the webs of the model to the support and retains the sectional geometry at the supports. The load cells were located on the cross beam to coincide with the axes of the top flanges of the model. The load cells do not restrain flexural rotation or warping of the section, but the end diaphragms do provide a restraint on warping.

Loading was applied directly to the top flanges of the

Figure 7. Details of model girders.

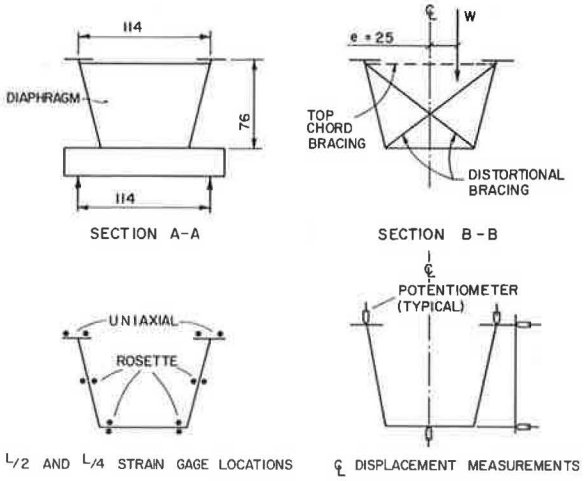

model to simulate the effects of the placement of concrete deck. The load was applied to the model through two sets of wiffle-tree systems arranged so that load was distributed to 16 equal point loads on each flange. The wiffle tree did not restrain horizontal displacement. The intensity of this equivalent uniform load could be varied between each flange so that the resulting line of action of the total load is eccentric to the centerline of the model and the eccentric loadings illustrated in Figure 2 can be modeled. For convenience, an eccentricity of 25 mm was used in testing (Section B-B in Figure 7).

Models were instrumented with strain gauges at the midspan and quarterspan points and with displacement potentiometers at midspan. The strain gauges (Figure 7) allow longitudinal and transverse strain measurements to be made, and the potentiometer readings yield vertical and horizontal displacements as well as rotations of the model.

Two series of model tests were carried out to examine (a) single members under combined torsional and flexural loading and (b) the response of interconnected members when the loaded member was restrained by bracing.

Response of Single Box Girders to Eccentric Loading

Both the open and the quasi-closed members (Figure 5) were studied under uniform eccentric loading. The eccentricity value chosen (25 mm) corresponds to an e_v/b ratio of 0.27, which is approximately twice the maximum e_v/b ratio noted for prototype structures during construction (Table 1).

Figure 8 illustrates the applied load versus midspan rotation response for both the open and the quasi-closed members. The location of the shear center (the center of rotation) for both the open and the quasi-closed members was found to lie outside the section and generally in the position shown in Figure 8. This result was expected for the open section; studies continue on calculation procedures for the location of the shear center of a quasi-closed box section.

The load-rotation response (Figure 8) of the open section is nonlinear but recoverable. The nonlinear response results from the increase in the torsional load resulting from the horizontal deflection of the relatively flexible thin-walled open section and the corresponding increase in torque (this is similar to the P - δ effect in eccentrically loaded slender columns). The initial portion of the load-deflection curve of the open section corresponds to the first-order analysis value, and the second-order analysis agrees favorably with the latter portion of the curve when the additional torque caused by the horizontal deflection of the member is included.

Figure 8. Rotation versus applied load for model girders.

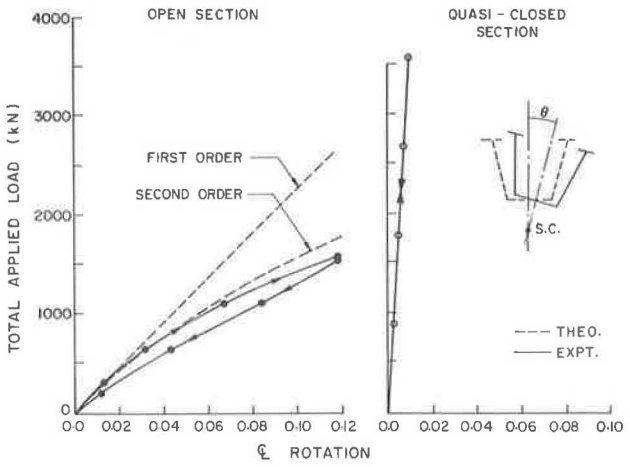

The load-rotation response of the quasi-closed member is linearly elastic and indicates that the torsional stiffness of this member is approximately 20 times that of the open-section member. The theoretical stiffness value for a quasi-closed section (8) is 50 times the open-section value. A similar ratio for theoretical to observed rotation has been observed for quasi-closed girders with span-to-depth ratios of 10 (7). Although the torsional stiffness value of the quasi-closed section is significantly larger than that of the open section, the reasons for the stiffness value for the quasi-closed section being less than the theoretical value are presently being examined.

The open-section member is subjected to two types of longitudinal stress: (a) flexural bending and (b) warping restraint. Because of the low torsional resistance of an open section, torsion in sections similar to that shown in Figure 4 is carried primarily by restrained warping. For the model section, the loading pattern, and the span studied, the total torque is resisted by both the warping restraint (warping torsional moment) of 85 percent and a St. Venant torsional moment of 15 percent. The longitudinal stresses developed by the warping torsional moment are significant for the extreme case of $e_v/b = 0.27$. Calculated values based on analyses developed by Vlasov (8) and Kollbrunner and Basler (9) were outlined by Harris (10). The results obtained from the mixed torsion analysis compare closely with Harris' observed values.

The longitudinal stress results for the quasi-closed section are basically those predicted by elementary beam theory. The quasi-closed section acts as a closed section and the torque is resisted by a St. Venant torsional moment.

Prototype Response

Because the results obtained from the model studies do not apply directly to a prototype structure, the prototype section (Figure 4) was analyzed for combined vertical concrete and formwork loading to develop an understanding of the stresses and displacements that might develop in such a structure. An eccentricity ratio (e_v/b) of 0.15 was used to determine an eccentricity of 285 mm for the vertical load from the centerline.

Section properties for the prototype span are as follows: Shear center distance below the geometric centroid = 1550 mm, $I_x = 5.58\ (10^{10})$ mm^4, $I_y = 1.13\ (10^{11})$ mm^4, and $I_\omega = 1.69\ (10^{16})$ mm^6. These properties were used in a mixed torsion analysis to give the following deformations caused by the eccentric line load (e_v = 285 mm) of 30 kN/m over an unsupported span length of 39.6 m: Midspan rotation = 0.0674 rad, midspan vertical deflection = 81 mm, and top-flange horizontal deflection at midspan = 157 mm. Girder movements of such a magnitude during construction would be unacceptable to the design engineer. Bracing of the torsionally open girder is necessary. The horizontal displacement of such a girder would be reduced by approximately $\frac{1}{20}$ if the eccentrically loaded open-section box girder were converted to a quasi-closed system or if the midspan section were restrained from rotating by suitable bracing.

Values for bending, warping, and total longitudinal stresses are shown in Figure 9 (in megapascals) for the loading case considered. The flexural longitudinal stresses are amplified appreciably when the open-section member is eccentrically loaded without intermediate

Figure 9. Longitudinal stress values for typical prototype structure.

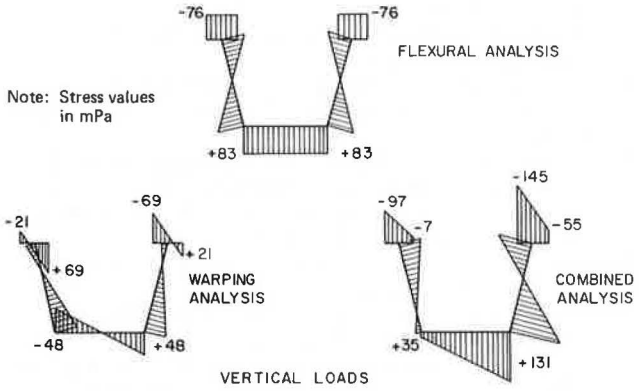

Figure 10. Interconnected model box-girder systems.

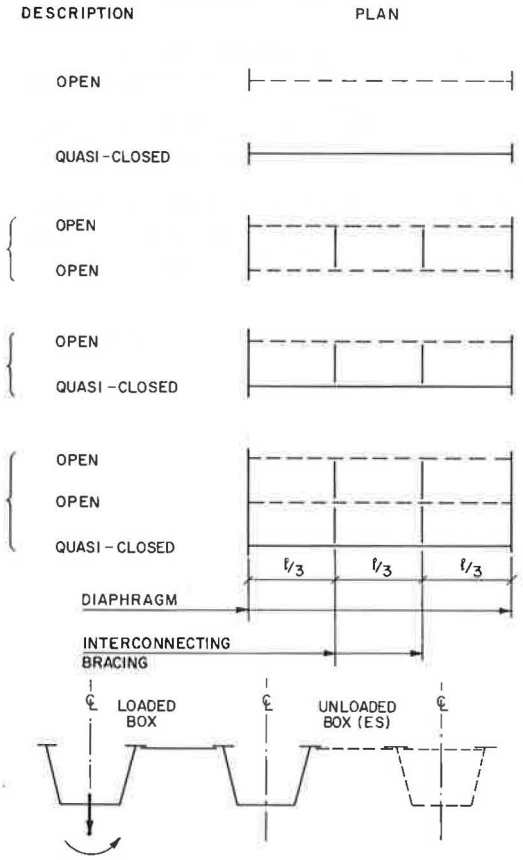

Figure 11. Relative horizontal displacements of open, quasi-closed, and interconnected box-girder systems.

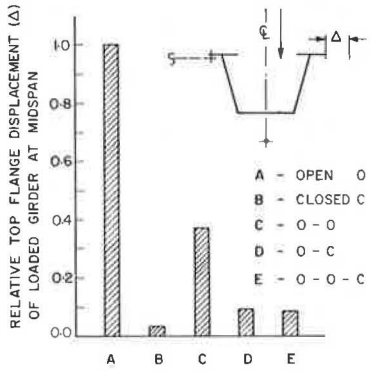

bracing within the span. An analysis of horizontal wind-force effects assumed a horizontal wind load of 1.2 kPa on the vertical face of the girder. The maximum wind stress is 20 MPa, approximately one-quarter of the gravity load bending stress. Wind-induced rotations are approximately one-third of the eccentric gravity load rotation.

Interconnected Model Box-Girder Studies

A series of tests was carried out on the box-girder arrangements shown in plan form in Figure 10. These were

1. A pair of connected open girders,
2. An open girder connected to a quasi-closed girder, and
3. A pair of connected open girders braced to a quasi-closed girder.

In each case one open box girder was loaded eccentrically and connected to the adjacent member(s) at the third points by a simple bar (Figure 10). Diaphragms were provided at the support points to ensure an adequate torsional restraint at the supports.

The loading case considered in Figure 10 assumes that only one girder is eccentrically loaded and that adjacent girders are subjected to a nearly concentric loading. The simple tie will not provide any restraint to torsional loading for the case of two connected open girders if the girders are eccentrically loaded so as to rotate in the same direction.

Figure 11 shows relative horizontal displacements measured at the elevation of the top flange for a single open and a single quasi-closed box girder as well as for three interconnected cases. Even in the case of two torsionally open box girders, a positive structural connection between two such girders will reduce horizontal displacements caused by eccentric loading. These horizontal displacements are reduced by more than 15 for systems that incorporate a single quasi-closed box girder as part of the multigirder system.

The single-tie bracing was chosen as the simplest and cheapest torsional restraint. Such a member may be retained in a completed structure without influencing the appearance.

DISCUSSION OF RESULTS

The rotation and horizontal movements observed during the construction of box girders that form part of a composite box-girder bridge structure can be attributed to a variety of torsional loadings, the sources of which include the concrete deck, wind, the finishing equipment, and the formwork. A torsional restraint at the supports is thus necessary to ensure overall stability of the member during construction. Additional bracing will frequently be necessary to minimize later movements and to ensure that large stresses are not built into the box-girder system. A similar conclusion was reached by Poellot (11).

Bracing should be supplied for a torsionally open cross section during construction to ensure that horizontal movements and associated longitudinal warping stresses are minimized. A number of possible bracing schemes are shown in preliminary form in Figure 10, and the relative deformations of these schemes under torsional loading are shown in Figure 11.

CONCLUSIONS

The probable causes of torsional loading of composite

box-girder bridge structures during construction have been discussed. These torsional loadings can be identified at the design stage so that structures with adequate torsional restraint at the supports can be proportioned by the design engineer. Model studies were supplemented by the results of mathematical analyses to predict the response of torsionally open and torsionally quasi-closed sections to combined flexure and torsion.

Bracing is obviously required between supports to maintain the stability of open-section members during construction. Geometrically and structurally stable configurations can be designed for construction loadings by using a variety of simple bracing schemes.

ACKNOWLEDGMENTS

The work described in this paper has been sponsored by the Canadian Steel Industries Construction Council (CSICC) as part of an annual research grants program. The assistance of CSICC and the council task group is acknowledged. A number of individuals have assisted with the project, and the help given by W. Rypstra, C. Harris, M. Daoud, and W. Mickenfielder is gratefully acknowledged. The work was carried out in the Models Laboratory, Department of Civil Engineering, University of Waterloo.

REFERENCES

1. Standard Specifications for Highway Bridges. AASHO, 10th Ed., 1969.
2. R. S. Fountain and A. H. Mattock. Composite Steel-Concrete Multibox Girder Bridges. Proc., Canadian Structural Engineering Conference, Canadian Steel Industries Construction Council, Toronto, 1968.
3. Standard Specifications for Highway Bridges. AASHO, 11th Ed., 1973.
4. Design of Highway Bridges. Canadian Standards Association, Toronto, CSA Standard S6-1974, July 1974.
5. A. H. Mattock. Development of Design Criteria for Composite Box Girder Bridges. In Developments in Bridge Design and Construction, Crosby Lockwood and Sons Ltd., 1972.
6. W. Rypstra. Model Testing of Steel Box Girders Under Construction Loading. Civil Engineering Department, Univ. of Waterloo, April 1975.
7. R. E. McDonald, Y.-S. Chen, C. Yilmaz, and B. T. Yen. Open Steel Box Sections With Top Lateral Bracing. Journal of Structural Division, Proc., ASCE, Vol. 102, No. ST1, Paper 11850, Jan. 1976, pp. 35-49.
8. V. S. Vlasov. Thin-Walled Elastic Beams. National Science Foundation and U.S. Department of Commerce, 1961.
9. C. F. Kollbrunner and K. Basler. Torsion in Structures. Springer-Verlag, New York, Heidelberg, and Berlin, 1969.
10. J. W. C. Harris. Torsion of Single Trapezoidal Box Girders. MASc thesis, Univ. of Waterloo, April 1976.
11. W. N. Poellot. Special Design Problems Associated With Box Girders. Proc., Specialty Conference on Metal Bridges, ASCE, St. Louis, Nov. 1974.

Publication of this paper sponsored by Committee on Steel Bridges.

Effects of Diaphragms on Lateral Load Distribution in Beam-Slab Bridges

Celal N. Kostem, Lehigh University
Ernesto S. deCastro,* Phillipine Construction Consortium Corporation, Quezon City

The effect of diaphragms on the lateral distribution of live load in simple-span beam-slab bridges with prestressed concrete I-beams and without skew is presented. The computer-based analysis used the finite-element method for two previously field-tested bridges with span lengths of 21.8 and 20.9 m (71.5 and 68.5 ft). The first part of the investigation dealt with the extent of the participation of the midspan diaphragms in lateral load distribution. It was found that the reinforced-concrete midspan diaphragms contribute only about 20 to 30 percent of their stiffness to load distribution. In addition, when all design lanes are loaded the contribution of the diaphragms is negligible. The second phase of the research dealt with the effect of the use of multiple diaphragms on lateral load distribution. Numerical comparisons were made for cases in which the superstructure had a midspan diaphragm and diaphragms at third, quarter, and fifth points. When the vehicle was located so as to produce maximum bending moment in the bridge, it was found that the increase in the number of diaphragms does not necessarily correspond to a more even distribution of loads at midspan. It was also found that, if all the design lanes are loaded, the contribution of diaphragms is negligible regardless of the number of diaphragms used.

Lateral distribution of live load in simple-span beam-slab highway bridges with prestressed concrete I-beams and without skew is one of the critical aspects in the design of these bridge superstructures. Until recently provisions for load distribution were far from realistic (2, 3, 6). Recent investigations have refined provisions for the lateral distribution of live load not only in right bridges but in skewed bridges as well (3,6). One of the major design issues for bridge engineers, however, remains unresolved: the contribution of midspan diaphragms (or third-span, depending on the span length) used in highway bridges.

This paper, which provides a summary of the findings of an extensive analytical research project on load distribution in beam-slab bridges (3), including sufficient qualitative information for use by designers, attempts to answer two basic questions:

1. In existing bridges with diaphragms, do the diaphragms fully participate in the lateral load distribution?
2. If the number of diaphragms is increased, will this lead to more uniform lateral distribution of loads at maximum moment section?

The studies used two beam-slab bridges with prestressed concrete I-beams. These bridges had previously been field tested by using a simulated HS20-44 vehicle that traversed several lanes, and the findings were reported (1, 2). Thus, before the research reported here was begun, sufficient experimental information was available to assess the reliability of a finite-element analysis. The diaphragms, because of their placement in the bridge superstructure, required the development of a detailed finite-element analysis scheme and a computer program as well as pilot studies that would verify that the results of the computerized analysis corresponded to actual results (4, 5).

TEST BRIDGES

The following basic bridge configurations were used in the study:

1. Lehighton Bridge—a six-beam bridge with a span length of 21.8 m (71.5 ft), a roadway width of 10.98 m (36 ft), and a beam spacing of 2.06 m (6.75 ft). PennDOT 24/45 beams were used. The superstructure had the standard safety curb and parapet on only one side. Diaphragms made of reinforced concrete, with dimensions of 254 by 711 mm (10 by 28 in), were located at midspan (2).
2. Bartonsville Bridge—a five-beam bridge with a span length of 20.88 m (68.5 ft), a roadway width of 9.75 m (32 ft), and a beam spacing of 2.44 m (8 ft). AASHO-II beams were used. Diaphragms made of reinforced concrete, with dimensions of 228 by 963 mm (9 by 34 in), were located at midspan. The structure had a safety curb and parapet on both sides (1, 6).

It should be noted that field testing of the bridges was not carried out within the framework of the reported research; the available data were only used to initiate the studies.

In all the analytical studies the standard HS20-44 vehicle was placed near the midspan of the bridge to produce maximum bending moments at the midspan. The analysis was then repeated by moving the vehicle laterally to simulate the effects of different lane loadings.

EFFECTIVENESS OF DIAPHRAGMS

In the actual bridge structure, the diaphragms are monolithic with the slab but are not fully continuous over the beams. The curbs, according to construction practice, are not made fully integral with the deck slab, and the parapets have a number of gaps along the span. Thus only a portion of the diaphragm section and the curb and parapet sections can be considered effective. Because the analytical studies indicated that a partially effective curb and parapet, whose cross-sectional area is 50 percent of the actual area, closely approximates bridge behavior (6), only half the area of the curb and parapet sections was used throughout this investigation.

In determining the effective section of the diaphragms, the bridge superstructures were first analyzed by means of truck loads on different lanes of the bridge that used the full diaphragm cross section. The resulting maximum moment was then used to compute the effective moment of inertia as defined by Section 9.5.2.2 of the American Concrete Institute (ACI) code (7). The effective moment of inertia for the Lehighton Bridge is computed to be 40 percent of the gross moment of inertia. Reanalysis has indicated that this percentage is still high. It is therefore estimated that only 25 to 35 percent of the gross moment of inertia participated in the lateral distribution of the live load (3).

The Bartonsville Bridge was also analyzed by using diaphragms that were 40 and 20 percent effective. Figure 1 shows a good agreement for 20 percent effective I_D (diaphragm composite moment of inertia). In this and the following figures, moment coefficient is the term used to denote the percentage of the total midspan moment carried by each beam. Further investigations, details of which are not included here, have indicated that the diaphragm is about 20 to 30 percent effective when all design lanes are not simultaneously occupied by the appropriate vehicles. If all design lanes are loaded, however, the contribution of the diaphragms in lateral load distribution is negligible (3).

Little is known about the effect of several lines of diaphragms across the span of a bridge superstructure. To investigate this, one, two, three, and four lines of diaphragms were used with a bridge that had dimensions similar to those of the Lehighton Bridge (Figure 2). For comparison purposes the same bridge was also analyzed without diaphragms. The influence lines for moment for five different cases are shown in Figure 3. Figure 4 shows the corresponding distribution factors for different beams and diaphragm arrangements. On the right side of Figure 4 s/k is shown; s is the beam spacing in feet and k = 5.5, the value specified in the current Standard Specifications for Highway Bridges of the American Association of State Highway Officials (AASHO) (8). (The AASHO values for load distribution are empirically derived in customary units; therefore, no SI equivalents are given.) The figure indicates the discrepancy between the distribution factor used in design and the actual behavior of the bridge with or without diaphragms. As the figure indicates, the bridge is assumed to have three traffic lanes (also referred to as design lanes). Because of the lane widths and the

Figure 1. Influence lines for moment for Bartonsville Bridge with partially effective diaphragms (beam B).

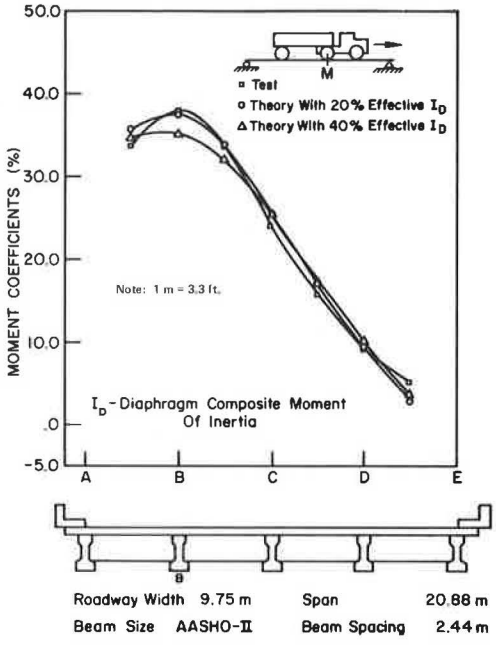

Figure 2. Diaphragm locations in six-beam bridge.

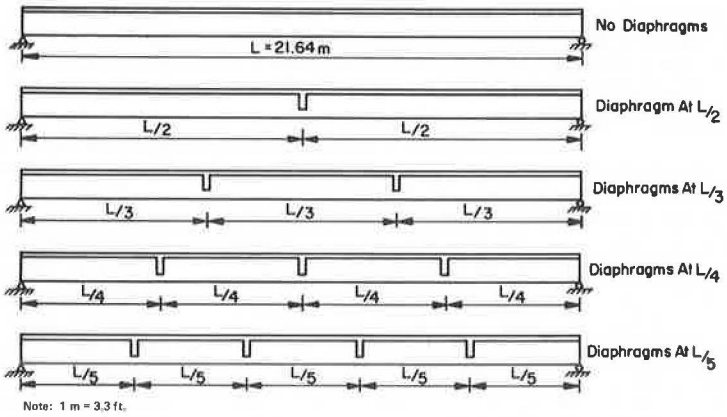

Figure 3. Influence lines for moment for six-beam bridge with and without diaphragms (beam C).

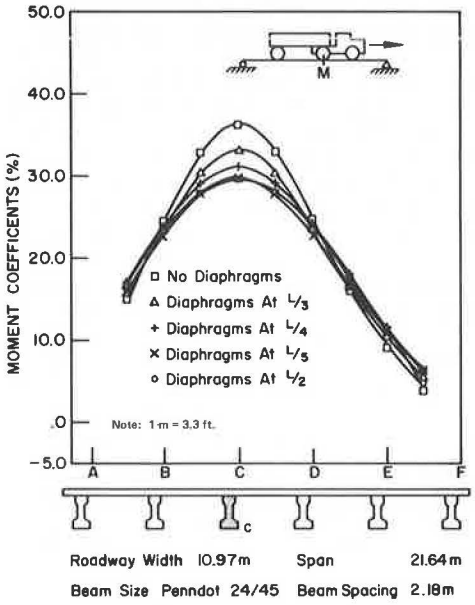

Figure 4. Distribution factors in six-beam bridge with and without diaphragms for one, two, or three loaded lanes.

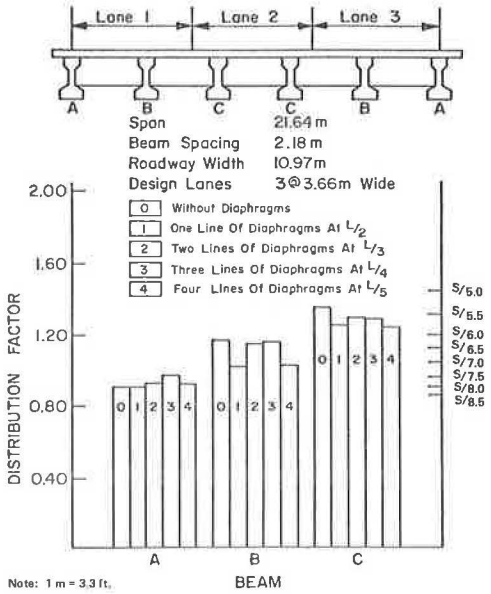

Figure 5. Distribution factors in six-beam bridge with and without diaphragms for one or two loaded lanes.

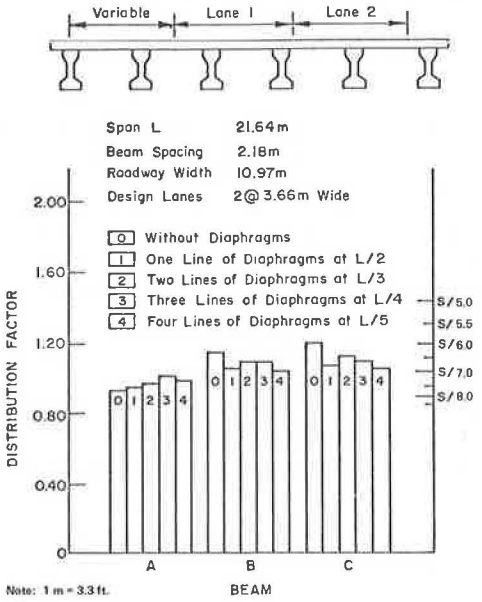

curb-to-curb width of the bridge, the lane locations are predefined. The maximum response can be achieved by simultaneous loading of either some or all of the lanes.

The analysis was also carried out for the same bridge for two adjacent lanes that can be moved in the transverse direction so as to obtain the maximum response for each beam. The results are shown in Figure 5. The difference in lateral load distribution for three-lane versus two-lane loading is marginal. The investigation was further extended to single-lane loading by positioning the lane so that maximum response was obtained for a given beam. The process was repeated for all the beams. Inspection of the results for the three-lane and two-lane cases (Figure 6) indicates that there is no noticeable change in the influence of diaphragms on lateral load distribution.

The following conclusions can be made.

1. For interior beams, the midspan diaphragm is the most effective arrangement for distributing load. The least effective arrangement is to use diaphragms at quarter points.
2. For the exterior beam, a larger participation in the distribution of load is induced by using diaphragms at quarter points.
3. In contrast to general belief, the contribution of

Figure 6. Distribution factors in six-beam bridge with and without diaphragms for one loaded lane.

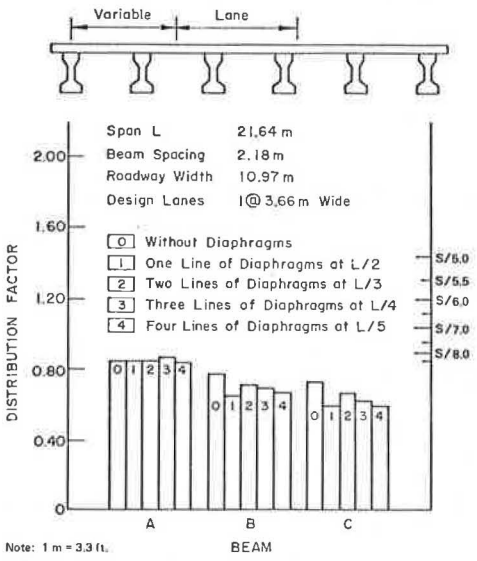

diaphragms to lateral load distribution is marginal regardless of the loading pattern.

APPLICABILITY OF FINDINGS

Although the types of bridges and loadings considered in this study may appear to restrict the applicability of the findings to only a limited number of bridges, the response of bridges with different span lengths and beam spacings will probably not vary substantially from the response of those investigated (3, 5). The scope of the study was not wide enough to permit the development of formulas to determine the participation of diaphragms in lateral load distribution. That would require a detailed parametric investigation.

Pilot studies have indicated that the response of bridges with moderate skew, i.e., a skew between 90° and 60° (90° being that of the right bridge), is very similar to that of right bridges. The findings reported here can thus be applied to bridges with moderate skew as well as to continuous right bridges (3). However, extrapolating the findings to simple-span or continuous bridges with large skew, e.g., a skew of less than 45°, would not be prudent.

CONCLUSION AND RECOMMENDATIONS

Midspan diaphragms are not fully effective in the lateral distribution of live load for beam-slab bridges with typical dimensions and construction details such as those encountered in design and construction practice. If more diaphragms are used and evenly spaced along the length of a bridge, the increase in the number of diaphragms does not necessarily correspond to a more uniform distribution of the load at maximum moment sections. Regardless of the extent of their participation or of how many of them are used, diaphragms make only a marginal contribution to the lateral distribution of live load. Finally, when all design lanes are fully loaded, the diaphragms do not contribute noticeably to the lateral distribution of live load; that is, the performance of the structure is analogous to that with no diaphragms.

This research has demonstrated that midspan diaphragms do not perform up to the expectations of bridge designers in the lateral distribution of live load. Further studies should investigate the cost-effectiveness of diaphragms to decide on their future use or discontinuance. It is generally believed that diaphragms can be an important factor in the uniform distribution of load when a superstructure is subjected to vehicle overload. This intuitive design rule must be verified before any discontinuance of the use of diaphragms in the future. Further studies should also consider the contribution of diaphragms to the response of bridges with large skew and continuous construction.

ACKNOWLEDGMENTS

Grateful appreciation is expressed to D. A. VanHorn for his continual assistance, guidance, and support during the conduct of the research. Parts of the investigation reported here were sponsored by the Pennsylvania Department of Transportation and the Federal Highway Administration, U.S. Department of Transportation. The contents of the paper reflect our views, and we are responsible for the facts and the accuracy of the data presented. The contents do not necessarily reflect the official views or policies of the sponsors. This paper does not constitute a standard, specification, or regulation.

REFERENCES

1. C. H. Chen and D. A. VanHorn. Static and Dynamic Flexural Behavior of a Prestressed Concrete I-Beam—Bartonsville Bridge. Lehigh Univ., Bethlehem, Penn., Fritz Engineering Laboratory Rept. 349.2, Jan. 1971.
2. C. H. Chen and D. A. VanHorn. Structural Behavior of a Prestressed Concrete I-Beam Bridge—Lehighton Bridge. Lehigh Univ., Bethlehem, Penn., Fritz Engineering Laboratory Rept. 349.4, Oct. 1971.
3. E. S. DeCastro and C. N. Kostem. Load Distribution in Skewed Beam-Slab Highway Bridges. Lehigh Univ., Bethlehem, Penn., Fritz Engineering Laboratory Rept. 378A.7, Dec. 1975.
4. E. S. DeCastro and C. N. Kostem. User's Manual for Program SKBRD. Lehigh Univ., Bethlehem, Penn., Fritz Engineering Laboratory Rept. 400.15, June 1975.
5. C. N. Kostem. Analytical Modeling of Beam-Slab Bridges. Proc., International Symposium on Folded Plates and Spatial Panel Structures, International Association for Shell and Spatial Structures, Udine, Italy, Sept. 1974.
6. M. A. Zellin, C. N. Kostem, and D. A. VanHorn. Structural Behavior of Beam-Slab Highway Bridges—A Summary of Completed Research and Bibliography. Lehigh Univ., Bethlehem, Penn., Fritz Engineering Laboratory Rept. 387.1, May 1973.
7. Building Code Requirements for Reinforced Concrete. American Concrete Institute. Detroit, ACI 318-71, 1971.
8. Standard Specifications for Highway Bridges. AASHO, 11th Ed., 1973.

Publication of this paper sponsored by Committee on Concrete Bridges.

**Mr. deCastro was with Lehigh University when this research was performed.*

Survey of Field and Laboratory Tests on Bridge Systems

Hota V. S. GangaRao, Department of Civil Engineering, West Virginia University

Field and laboratory tests were conducted on the behavior of several short-span bridge systems: orthotropic deck; composite box girder; composite U-beam superstructure; precast, prestressed concrete deck planks; and concrete box girder. The results are critically reviewed from the viewpoint of fabrication, erection, performance, and first cost. Because the test results consistently proved that the current AASHO transverse load distribution factors are very conservative, tentative distribution factors are suggested for the interior and exterior girders of bridges with two or more lanes.

Systems construction may be defined as a schematic technique for a well-conceived, mechanized operation that uses optimal sizes of mass-produced structural components and requires minimal field labor (i.e., makes efficient and maximum use of available human and material resources). It may be described as a concept that signifies the thinking and operation process of which the structure is a part. The process consists of an interrelation of function, design, production, erection, and economics in which flexibility of arrangement is one of the most important criteria. Terms such as prefabrication, industrialized building, and modular construction are also used to describe these aspects.

Because the systems construction of bridges is different from conventional construction methods, extensive research and development and large-scale field testing are required to (a) develop speedy, economical, foolproof methods of construction by assembling various components on a "streamline" basis; and (b) ensure that the response of the final assemblage should be at least as good as that of a monolithically built bridge structure. In addition, adequate constraints based on theoretical criteria and previous experience, which are contained in national building codes, are needed to ensure safety and satisfactory serviceability of a new bridge system.

The most important objective of this paper is to examine the behavior of several superstructural bridge systems tested in the field and the laboratory. In addition, basic limitations on and possible modifications of bridge-system construction are discussed in relation to fabrication, transportation, erection, performance, and first cost. The discussion is limited to short-span bridge superstructures [3 to 23 m (10 to 75 ft)] that lend themselves to a modular type of construction. Although many excellent sources exist on the general subject of bridge testing (1, 6, 7, 13), a literature review is not attempted here because most of these publications do not deal with systems concepts of bridges.

TESTS

Tests were performed on the following modular bridge units: (a) orthotropic deck systems; (b) composite box-girder systems; (c) composite U-beam superstructure; (d) precast, prestressed concrete deck planks; and (e) concrete box girders. The tests and their results are discussed below.

Orthotropic Deck Systems

In 1964 Bethlehem Steel Corporation built an experimental bridge at its Sparrows Point, Maryland, site (4, 24). The system used a basic modular unit with the deck assembly and main girder. Dimensions of these units varied from 6 to 24.4 m (20 to 80 ft), in increments of 3 m (10 ft). Figure 1 shows details of the system. A similar system with two continuous spans (Figure 2) was built by the Michigan Department of State Highways as a part of Crietz Road over I-496 (18).

In this research the static behavior of a single unit of the Bethlehem Steel bridge was studied by placing the unit in a test rig in the laboratory. The entire width of the deck assembly acted uniformly in resisting overall bending in the unit, and the field test results showed how the wheel-load distribution factor varied with the width of the bridge. For example, the distribution factor was reduced from 97 to 68 percent of the American Association of State Highway Officials (AASHO) code value (2) by doubling the width of a single deck unit. In addition, test results revealed that the number, the type, and the positioning of vehicles had an influence on the distribution factors. In the field tests critical stresses were observed at the bottom of a longitudinal rib that was passing over the floor beam. A comparison of computed and measured strains and deflections of various components such as main girders, ribs, floor beams, and deck of the Crietz Road bridge indicated that the design assumptions are very conservative and that all the measured values are well below the calculated ones. For example, the maximum calculated transverse strain and relative deflection in the deck, based on the uniform wheel-load distribution over a rectangular area, were about 700 μm/m (μin/in) and 1.52 mm (0.06 in) respectively, whereas in the test results they were of the order of 100 μm/m (μin/in) and 0.25 mm (0.01 in).

It is interesting to note, from tests on the Bethlehem Steel bridge, that dual-tire stresses are about 14 percent less than the theoretical values computed from the design manual of the American Institute of Steel Construction (3). However, single-tire stresses were about 8 percent higher than theory. A similar phenomenon was observed in the case of the Crietz Road bridge. The impact factor for the girders of the Bethlehem Steel system was found to be about 0.1, whereas the AASHO code (2) specifies a value of 0.3. However, the impact factor for the deck and the floor beams directly under the wheel agreed with the AASHO specifications. A similar trend was noted in the Crietz Road bridge: Dynamic runs at speeds of about 30.2 km/h (20 mph) gave peak strains and deflection values approximately 10 to 15 percent higher than the static readings.

Although the field performance of asphalt surfacing with epoxy membrane in the Bethlehem Steel system was reported to be satisfactory over a 3-year period, recent reports, including the Crietz Road bridge records (18), have proved that the wearing surfaces in general did not function satisfactorily. However, a comprehensive study by a Pennsylvania firm on the performance aspects of wearing surfaces revealed that rubberized asphalt surfacing with epoxy membrane performed well during field and laboratory testing. The product is supplied only by Adhesive Engineering Company of San Carlos, California, and the complete installation costs may vary from $30 to $33/m^2 ($36 to $40/yd^2). Additional information on paving practices for wearing surfaces on orthotropic steel bridge decks can be found elsewhere (18).

Figure 1. Bethlehem Steel experimental orthotropic system.

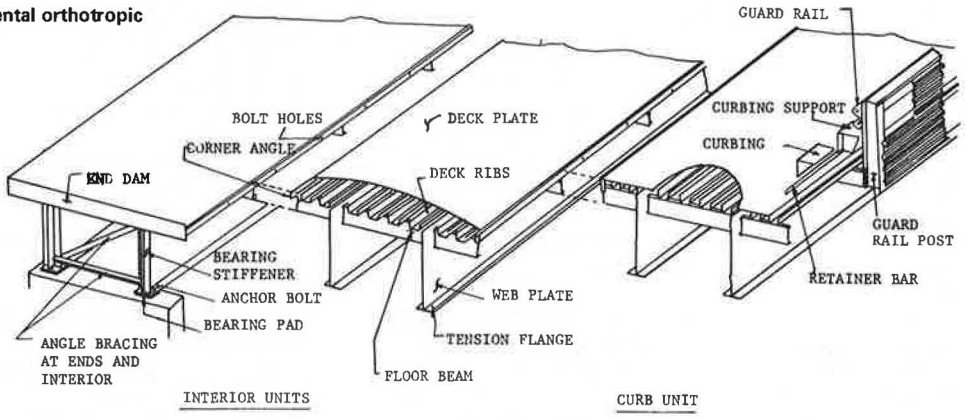

Figure 2. Deck section of continuous orthotropic steel plate deck bridge.

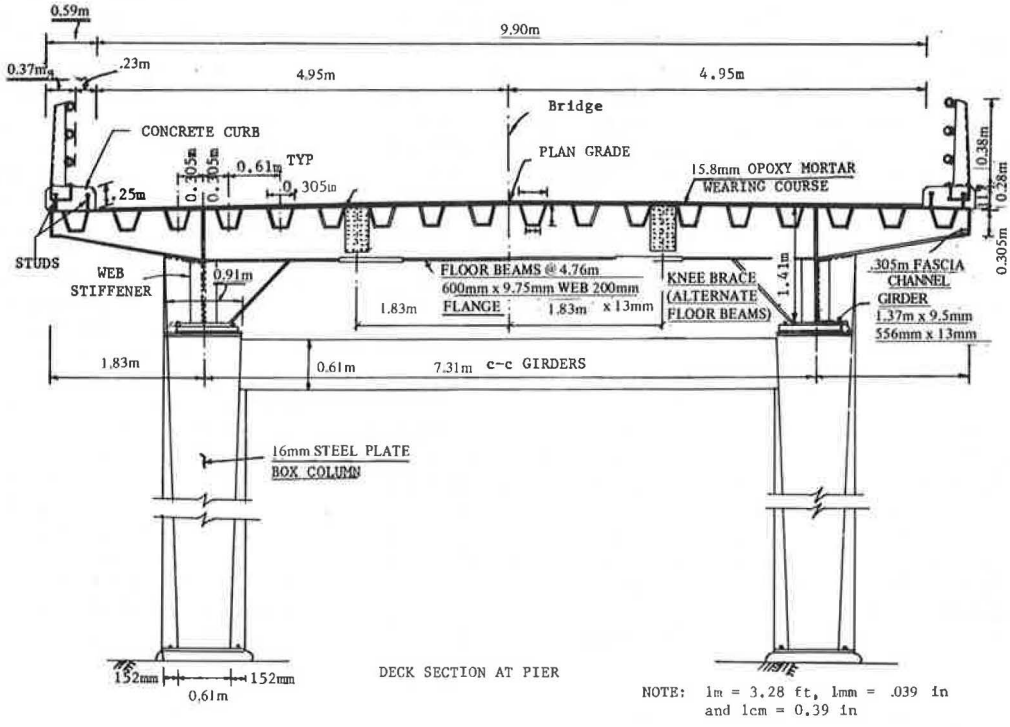

Figure 3. Typical composite box-girder bridge with prototype and model dimensions.

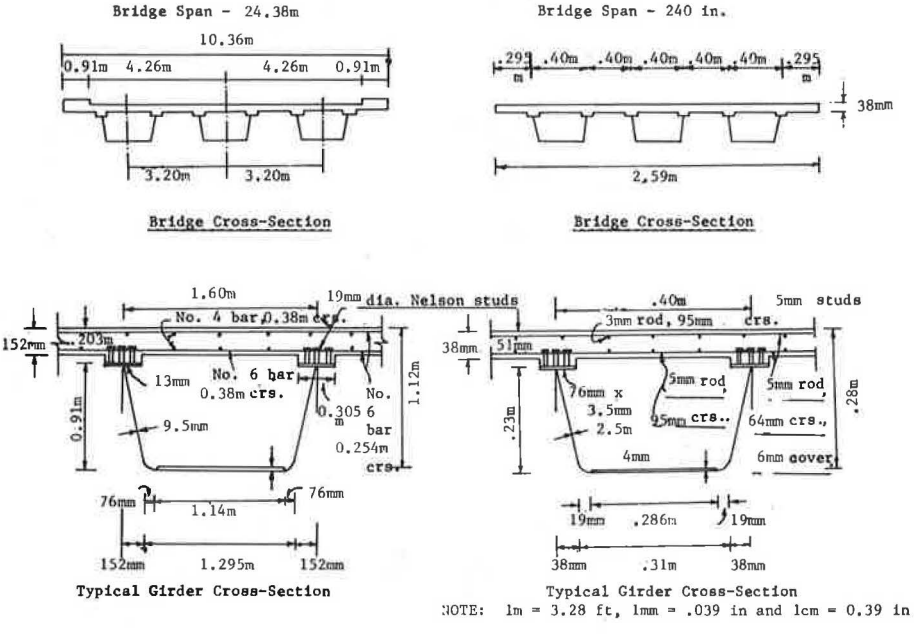

Composite Box-Girder System

Figure 3 shows a general view of a bridge with a composite box-girder system as well as the details of a two-lane, 24.4-m (80-ft) span prototype system with three box units and a corresponding quarter-scale model. The bridge was designed (12) for an HS20-44 loading with a distribution factor of S/6.5, instead of S/5.5 as suggested by AASHO (2) (S is defined as the girder spacing in feet). (The AASHO values for load distribution are empirically derived in customary units; therefore, no SI equivalents are given.)

The model was tested under concentrated loads and for simulated truck loads. Transverse influence lines for midspan deflection and the average strain (at the bottom plate) of each girder were constructed from these load tests. When test results were compared against the folded plate theory, based on Fourier series expansion, there was good agreement. According to Johnston and Mattock (12), the calculated transverse distribution of loads was in close agreement with the measured distribution. They also found that the measured maximum loads carried by exterior and interior girders were equivalent to the load distribution factors of S/6.91 and S/6.48 respectively, which agreed closely with the assumed distribution factor of S/6.5. Finally, Johnston and Mattock concluded that the transverse load distribution factors derived from the AASHO code were very conservative and that the most economical composite box-girder arrangement was one box-girder system for each lane of traffic.

U-Beam Superstructure System

A composite U-beam bridge superstructure was developed in the United Kingdom as well as in the United States. Typical cross-sectional details of the test specimens are shown in Figure 4. The Missouri system developed in the United States (20, 21) was tested with single and multiunit beams for single concentrated load as well as simulated AASHO HS20-44 truck loads. Field tests of the multiunit British system (8, 14) were conducted for eccentrically loaded HB vehicles. Single-unit test results—i.e., continuous and linear strain distributions through the depth of the test specimens at various load levels and deflections based on an idealized composite action of the Missouri system (19)—indicated complete composite action between the U-beam and the cast-in-place deck.

The Guyon-Massonnet load distribution theory (16) was used to predict lateral distribution of moments and deflections of the multiunit system. The measured and calculated results are given by Salmons and Mokhtari (21). As was observed in earlier investigations, the distribution characteristics were found to change with the position of the applied load. The maximum wheel-load distributions from the tests were compared with the distribution factors from the AASHO code, and it was found that the AASHO code results were very conservative. Since the multiunit system was tested to failure, Salmons and Mokhtari (21) have observed ductile behavior of the whole unit in which the ultimate deflection was more than 20 times the elastic deflection.

As a result of extensive experimental and theoretical investigation of the U-beam system, Cusens and Rounds (10) recommended for design purposes the finite strip method, which, when it was compared with the load distribution method or the orthotropic theory, was found to be accurate and economical. Cusens and Rounds observed initial cracking and final collapse at 1.68 and 3.73 times the design loads respectively, and the crack pattern indicated effective distribution of the load between the girders. In addition, transverse load distribution through the top slab, taken from the strain readings between the slab and the beam webs, appeared to be adequate. However, the authors recommend further experimental work to study the effectiveness of various types of beam-slab joints and their influence on the overall behavior of bridges.

In spite of a detailed cost analysis by Salmons and Kagay (20) that found the U-beam system to be economical for 10 to 24.4-m (30 to 80-ft) span ranges, recent correspondence with the Missouri State Highway Commission revealed that, because this system is not economically competitive with some of the existing ones, its use has been discontinued.

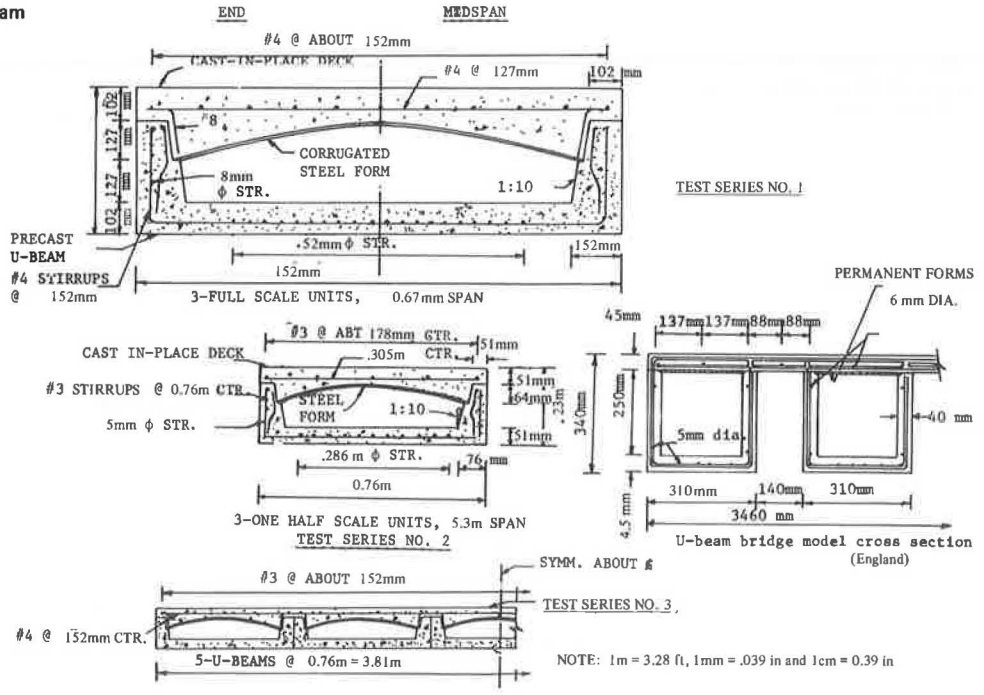

Figure 4. Cross-sectional details of U-beam models.

Figure 5. Typical elevation and cross section of concrete bridge slabs.

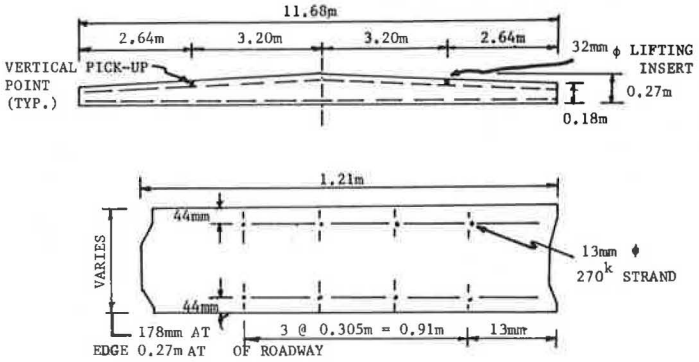

Figure 6. Joint shapes.

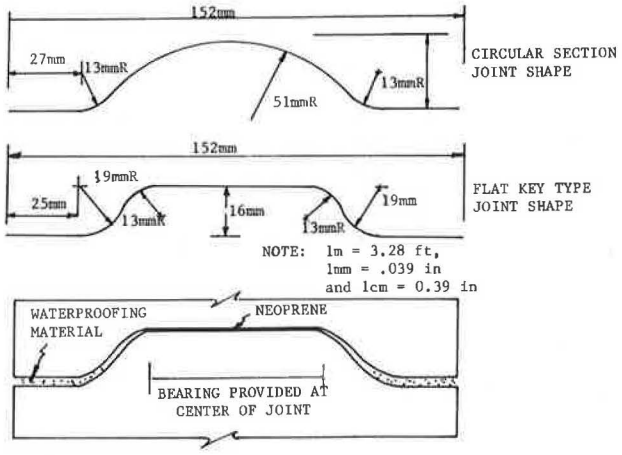

Precast, Prestressed Concrete Slab Units

A system of precast, prestressed concrete slab units placed on stringers has been found to be feasible and easy to erect compared with conventional methods. Two such systems were built in 1970 on Ind-37 and Ind-140 (14); the cross-sectional details for the slabs are shown in Figure 5. Features common to both bridges included the following:

1. Precast slabs as long as the road width and 2.4-m (8-ft) sections were placed on longitudinal stringers.
2. A tongue and groove shear keyway ran the entire width of the slab to join individual units. Joints were sealed by bonding a 0.16 × 12.1-cm (0.06 × 4.75-in) neoprene strip that ran along the slab joint.
3. Slab units were anchored to the girders by 115-RE-F railroad clips and 1.91-cm-diameter (0.75-in) bolts.
4. After slab units were placed on stringers, they were posttensioned along the bridge length and anchor bolts were tightened at a specified torque level.

Cracks running transverse to the slabs appeared near the joint during and after posttensioning operations as a result of irregularities in the slab crown section that caused poor fit between adjacent units and possibly because of the application of excessive prestressing force. Although the Indiana systems seem to have performed well over a 4 or 5-year period, the following maintenance problems were noted:

1. Leaking of joints—Of two kinds of joint sealants, Dupont's Imron sealant proved to be superior to the liquid polyurethane sealant. It was advised that the manufacturer's directions be carefully followed during the application of the joint sealant.
2. Loosening of bolts—Bolts clamping slabs to beams worked loose. They had originally been tightened to 67.75-J (50-ft-lb) torque; they were retightened to a torque of 169.37 J (125 ft-lb).

To alleviate the spalling of concrete near the joint, three different joint configurations, shown in Figure 6, were tested in the laboratory under repeated loads; the joint type recommended is shown at the bottom of the figure. The bearing was limited to the flat center portion of the joint, which eliminated the spalling of corners. Joint sealant of sufficient thickness was provided in the gap above and below the flat center part of the joint to prevent leakage of water.

Concrete Box-Girder System

A large number of reinforced or prestressed concrete box-girder bridges were built in California and Pennsylvania during the past decade (9) because they had proved to be durable and economical, particularly in spans of 18.3 to 30.5 m (60 to 100 ft). Since the construction of a number of these systems in the state of California, an extensive investigation has been conducted on the structural behavior of the two-span, reinforced-concrete, box-girder bridge model (5, 23). Details of the model are shown in Figure 7.

Three different analytical methods were used to mathematically model the multicell box-girder system. The modeling approach is based on idealizing the system into one- and two-dimensional elements and solving for the displacements and forces within the elastic range by finite-element techniques (15, 17). Scordelis and others (23) concluded that the transverse distribution of the total moment at a section, in terms of percentage to each girder, was predicted accurately at working stress levels for single point loads and uniform loads across the width of the bridge. Although premature failure was observed in the undiaphragmed span, both undiaphragmed and diaphragmed spans exhibited excellent load distribution characteristics under ultimate load conditions with a factor of safety of four against live load overloads. The magnitude and distribution of live load deflections were also predicted accurately when theoretical values based on uncracked sections were multiplied by a factor of about 1.5 to account for cracking (15). Interestingly, the total reaction and the total moment at any section were found to be independent of the transverse position of the point loads.

LOAD DISTRIBUTION FACTORS

The AASHO code (2) recognized through experimental results that the transverse load distribution of a stan-

Figure 7. Dimensions and cross section of box-girder bridge model.

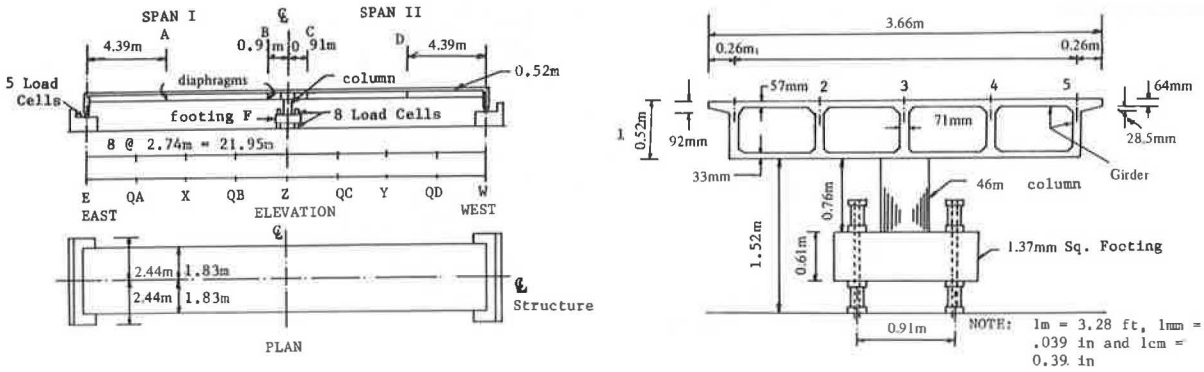

Figure 8. Load distribution factor versus flexural parameter.

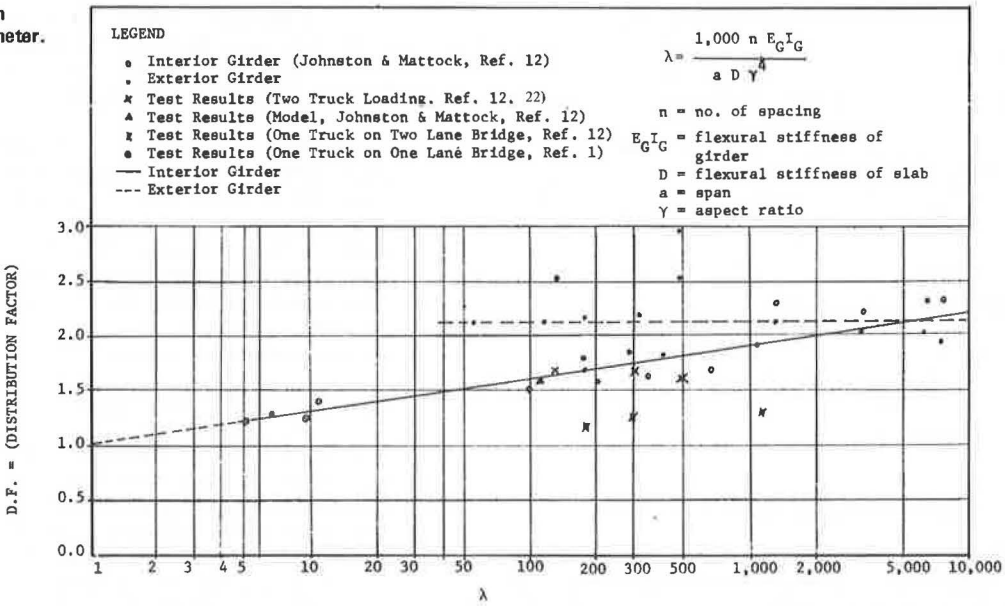

dard slab-stringer system is different from that of a spread box system, a composite box-girder system, or even the multibeam superstructure system. However, a comparison of experimental distribution factors with those from the orthotropic theory and the harmonic analysis revealed no consistent agreement with either one of the analytical methods (22). This is substantiated by the fact that the experimental and AASHO load distribution factors of a two-lane bridge are 2.54 and 1.76 respectively (22). In addition, test results for a three-span, two-lane bridge (13) yielded a maximum distribution factor of 0.389, whereas the AASHO distribution factor for a corresponding two-lane bridge was 1.667.

Variation of the transverse load distribution factor with a nondimensional flexural parameter (λ), based on existing experimental information, is plotted in Figure 8 (25). The distribution factor varies exponentially with λ for interior girders, and the same variation is a constant of 2.13 for exterior girders. Because the distribution in Figure 8 does not represent a wide range of systems or types of construction, a simple mathematical relation can be suggested only after conducting additional tests. It should be noted that, for composite steel box-girder bridges, the value of I_s in the flexural parameter (λ) is computed by idealizing the box as two wide-flange sections in which half of the bottom-flange effectiveness goes to each wide-flange unit.

CONCLUSIONS

Test results for orthotropic bridge systems revealed that dual-tire stresses are less severe than those caused by single tires and that the impact factor for girders was about one-third of the suggested AASHO value although the local effects on the deck and the floor beams reached about 30 percent of the equivalent static load. Precast, prestressed concrete slab units appeared to lend themselves to renovation of commonly built deck-stringer bridges. However, a special joint with a flat center portion between the precast units was found to be essential to preventing spalling during posttensioning operations.

Laboratory tests of composite and all-concrete box-girder systems indicated a better transverse load distribution relative to the other systems discussed. In addition, the box system, as observed in service in states like Pennsylvania and California, was found to be durable and economical. Although the concrete U-beam girder system with cast-in-place deck provided complete composite action and behaved as a box system, its use has been discontinued for economic reasons. The experimental results yielded better transverse load distributions for deck length-to-width ratios of the order of 1:2. The transverse distribution was also found to be a function of the number, the type, and the positioning of

loads. Finally, exponential variation of the transverse load distribution factor with the flexural parameter (λ) is tentatively suggested for interior girders, and a constant distribution factor of 2.13 is recommended for exterior girders.

REFERENCES

1. The AASHO Road Test: Report 2—Materials and Construction. HRB, Special Rept. 61B, 1962.
2. Standard Specifications for Highway Bridges. AASHO, 11th Ed., 1973.
3. Design Manual for Orthotropic Steel Plate Deck Bridges. American Institute of Steel Construction, 1963.
4. Modular Steel Bridges—Data and Specifications. Bethlehem Steel Corp., Booklet 2268.
5. J. G. Bouwkamp, A. C. Scordelis, and S. T. Wasti. Ultimate Strength of Concrete Box Girder Bridge. Journal of Structural Division, Proc., ASCE, Vol. 100, No. ST1, Paper 10293, Jan. 1974, pp. 31-49.
6. E. G. Burdette and D. W. Goodpasture. Comparison of Measured and Computed Ultimate Strengths of Four Highway Bridges. HRB, Highway Research Record 382, 1972, pp. 38-49.
7. E. G. Burdette and D. W. Goodpasture. Tests to Failure of a Prestressed Concrete Bridge. Journal of Prestressed Concrete Institute, May-June 1974, pp. 93-102.
8. E. C. Chaplin and others. The Development of a Design for a Precast Concrete Bridge Beam of U-Section. Structural Engineer, Vol. 51, No. 10, Oct. 1973, pp. 383-388.
9. Standards for Bridge Design (Adjacent Box Beam Prestressed Concrete Structures). Pennsylvania Department of Transportation, Harrisburg, BD-211, March 1973.
10. A. R. Cusens and J. L. Rounds. Tests of a U-Beam Bridge Deck. Structural Engineer, Vol. 51, No. 10, Oct. 1973, pp. 377-382.
11. A. W. Hendry and L. G. Jaeger. Load Distribution in Highway Bridge Decks. Proc., ASCE, Vol. 82, No. ST4, 1956, pp. 1023-1-1023-48.
12. S. B. Johnston and A. H. Mattock. Lateral Distribution of Load in Composite Box Girder Bridges. HRB, Highway Research Record 167, 1967, pp. 25-30.
13. H. L. Kinnier and F. W. Barton. A Study of a Rigid Frame Highway Bridge in Virginia. Virginia Highway and Transportation Research Council, VHTRC 75-R47, April 1975.
14. P. K. Kropp. Use of Precast-Prestressed Concrete for Bridge Decks. Purdue Univ. and Indiana State Highway Commission, Joint Highway Research Project, Rept. 7, March 1973.
15. C. S. Lin and A. C. Scordelis. Computer Program for Bridges on Flexible Bents. Univ. of California, Berkeley, Structural Engineering and Structural Mechanics Rept. 71-24, Dec. 1971.
16. C. Massonnet. Methods de Calculdes Points a Poutres Multiplies Tenant Compte de leur Resistance a la Torsion. International Association for Bridge Structural Engineering, Zurich, Vol. 10, 1950, pp. 147-182.
17. C. Meyer and A. C. Scordelis. Computer Program for Non-Prismatic Folded Plates With Plate and Beam Elements. Univ. of California, Berkeley, Structural Engineering and Structural Mechanics Rept. N-23, Dec. 1971.
18. J. E. Risch. Final Report of Experimental Orthotropic Bridge, Crietz Road Crossing Over I-496. Michigan Department of State Highways, Nov. 1971.
19. J. R. Salmons. Study of a Proposed Precast-Prestressed Composite Bridge System. Univ. of Missouri, Columbia, Missouri Co-operative Highway Research Program Rept. 69-2, Final Rept., May 1970.
20. J. R. Salmons and W. J. Kagay. The Composite U-Beam Bridge Superstructure. Journal of Prestressed Concrete Institute, Vol. 16, No. 3, May-June 1971, pp. 20-32.
21. J. R. Salmons and S. Mokhtari. Structural Performance of the Composite U-Beam Bridge Superstructure. Journal of Prestressed Concrete Institute, Vol. 16, No. 4, July-Aug. 1971, pp. 21-33.
22. W. W. Sanders and H. A. Elleby. Distribution of Wheel Loads on Highway Bridges. NCHRP, Rept. 83, 1970.
23. A. C. Scordelis, J. G. Bouwkamp, and S. T. Wasti. Structural Response of Concrete Box Girder Bridge. Journal of Structural Division, Proc., ASCE, Vol. 99, No. ST10, Paper 10069, Oct. 1973, pp. 2031-2048.
24. G. W. Zuurbier. Testing of a Steel Deck Bridge. HRB, Highway Research Record 253, 1968, pp. 21-24.
25. N. B. Taly and H. GangaRao. Compendium of Superstructural Bridge System. Civil Engineering Department, West Virginia Univ., Morgantown, WVDOH-50-Interim Rept. 8, Oct. 1976.

Publication of this paper sponsored by Committee on Dynamics and Field Testing of Bridges.

Highway Bridge Vibration Studies

John T. Gaunt, Trakool Aramraks, Martin J. Gutzwiller, and Robert H. Lee,
Purdue University

The results of acceleration studies of highway girder bridges are presented. Deflection limitations and maximum span-depth ratios used in present bridge design codes do not necessarily ensure the comfort of bridge users. Vertical accelerations have been shown to be significant in producing adverse psychological effects on pedestrians and occupants of stopped vehicles. The effects on bridge accelerations of major bridge-vehicle parameters, including the properties of the bridge and the vehicle as well as the initial conditions of the roadway, were investigated analytically and compared to criteria for human response. Numerical solutions are obtained from a theory in which the bridge is idealized as a plate continuous over flexible beams for simple-span bridges and as a continuous beam with concentrated point masses for two- and three-span bridges. The vehicle is idealized as a sprung mass system. The results indicate that, for simple-span bridges, accelerations that might psychologically disturb a pedestrian are primarily influenced by bridge-span length, vehicle weight and speed, and especially roadway roughness. Less significant factors are

girder flexibility and transverse position of the vehicle. For the two- and three-span continuous bridges studied, roadway accelerations exceeded the recommended limit for comfort only when the effects of surface roughness were included.

This investigation is aimed at obtaining a better understanding of highway bridge vibrations by studying the effects of varying some of the parameters of the vehicle-bridge system. It is hoped that the results of the study will ultimately be useful in establishing design criteria that will directly regulate dynamic response characteristics.

Dynamic response is not specifically mentioned in current bridge design codes (1). Instead, deflection limitations and maximum span-depth ratios are specified in the hope of controlling vibrations; these code provisions do not, however, attack the problem directly. Other effects, such as acceleration and jerk, are known to be more significant than maximum deflection in producing adverse psychological reactions to bridge vibrations (complaints of disturbing bridge motions come primarily from pedestrians and from persons in halted vehicles).

The economical use of modern, high-strength steels may also be hindered somewhat by present code limitations if the design is controlled by deflection rather than strength requirements. Significant savings might be possible in the design of high-strength steel girder bridges if the somewhat arbitrary restrictions were replaced by dynamic response criteria.

The dynamic response of both simple-span and two- and three-span continuous-girder bridges has been investigated. The most successful recent analytical studies are those by Oran and Veletsos (2) for simple-span highway bridges and Veletsos and Huang (3, 4) for multispan continuous highway bridges. The computer programs developed by these researchers have been used, with some minor modifications, in this study.

Several reports (5, 6, 7, 8, 9) have discussed criteria for human response to vertical vibration. The report by Wright and Walker (5), which summarizes the effects of bridge flexibility on human response, suggests that human sensitivity to vibrations is most closely related to acceleration in the usual frequency range for multibeam highway bridges. Because most tests of vertical vibration perception have been conducted for harmonic vibrations, Lenzen (7) has suggested that the tolerance level be multiplied by a factor of 10 for short-duration peak accelerations. Wright and Walker (5) suggest a maximum acceleration magnitude of 2.54 m/s^2 (100 in/s^2) for comfort.

Because of the strong relation between acceleration and vibration perception, this study focuses on the variation of maximum bridge accelerations with significant bridge-vehicle parameters such as girder span and flexibility, vehicle weight and speed, axle spacing, and roadway roughness.

SIMPLE-SPAN BRIDGES

Method of Analysis

The method of analysis used in this paper for the dynamic response of simple-span, multigirder highway bridges was developed by Oran and Veletsos (2). Their computer program has been modified somewhat for this study to provide more acceleration information and to increase the capabilities for both input and output.

In this analysis the bridge is represented as a plate continuous over flexible beams. Both bending and torsional stiffnesses of the beams are considered, but composite beam-slab action is not. The major steps of the analysis are (a) determining the instantaneous values of the interacting forces between the vehicle and the bridge and the inertia forces of the bridge itself and (b) evaluating the deflections and moments produced by these forces. The second step, which is a problem of statics alone, is solved by a combination of energy principles and the Levy method of analysis for simply supported rectangular plates. Vertical deflections are represented in the form of a double Fourier sine series. The solution has been shown to converge fairly rapidly so that only a limited number of terms are required.

Strain and potential energy of the system are written in terms of the deflections. Enforcing the condition that the total energy must be a minimum yields a set of equations for determining the Fourier coefficients, which can then be substituted into the appropriate moment and deflection expressions.

In the dynamic analysis, the mass of the slab is assumed to be uniformly distributed and the mass per unit length of each beam is assumed to be constant. The vehicle is represented by a single-axle, two-wheel loading that consists of a sprung mass and two equal unsprung masses. The springs are assumed to be linear elastic and to have equal stiffnesses. Damping has been neglected for both the vehicle and the bridge. The vehicle is assumed to move at constant velocity. The dynamic deflection configuration of the structure is represented by a Fourier series with time-dependent coefficients.

Again the total energy of the system can be written in terms of the displacement coordinates and their derivatives. Dead load deflections and unevenness of the roadway surface are included in the appropriate energy terms. The equations of motion are formulated by applying Lagrange's equation.

The procedures used to evaluate the dynamic response of the bridge-vehicle system can be summarized as follows:

1. The governing differential equations of motion are solved by means of a step-by-step method of numerical integration to determine the generalized coordinates and their first two derivatives. The time required for the vehicle to cross the span is divided into a number of small intervals, and the governing equations are satisfied only at the ends of these intervals by means of an iteration scheme.
2. The interacting forces between the vehicle and the bridge and the inertia forces of the bridge are evaluated.
3. The dynamic deflections and the bending moments induced in the bridge are determined from the dynamic forces acting on the bridge.

Acceleration Studies

The purpose of this investigation is to study the major parameters that affect the accelerations of simple-span highway bridges under moving loads. The study is based on the previously described analysis method and computer program. Bridge data were taken from Standard Plans of Highway Bridge Superstructures of the U.S. Bureau of Public Roads (10). The study is restricted to steel I-beam bridges with noncomposite reinforced concrete decks. The effect of side curbs is not taken into account.

Parameters that affect bridge accelerations can be classified as (a) bridge parameters, such as beam span and stiffness; (b) vehicle parameters, such as velocity and transverse position of the wheels; and (c) construction parameters, such as roadway roughness. The accuracy of the analysis depends, of course, on such solution parameters as the number of terms chosen for the deflection series expressions and the number of integra-

tion steps. For the simple-span bridge study, satisfactory convergence was obtained by dividing the time required for the vehicle to cross the span into 400 integration steps. The total computer time required to obtain the response of a bridge with a span of 18 m (60 ft) is approximately 150 s on a CDC 6500 computer.

Bridge Parameters

The effect of span length on maximum midspan accelerations is shown in Figure 1. The bridges are standard designs for an HS20-44 loading with a 13-m (44-ft) roadway width. Six steel beams support the 190-mm (7.5-in) reinforced concrete deck. Beam sizes range from W21×62 for the 6-m (20-ft) span to W36×300 for the 21-m (70-ft) span. Corresponding fundamental bending frequencies are 16 and 4 Hz.

The vehicle is represented by a single-axle, two-wheel, 32 667-kg (72 000-lb) loading that moves across the span at a constant velocity of 96 km/h (60 mph). The stiffness of each tire spring is 1051 kN/m (6000 lbf/in). Unsprung loads and damping are neglected. As the vehicle travels along near the edge of the bridge, the inside wheel is over beam 2. The exterior beams are shown to have somewhat higher midspan accelerations than the interior beams. Figure 1 also shows a definite increase in maximum accelerations for the standard bridge designs as the span is decreased.

Figure 2 shows the variation of the midspan acceleration of each beam as the vehicle crosses an 18-m (60-ft) span. Accelerations of beam 1 and beam 6 are out of phase all the time. Note that the maximum acceleration of beam 1 occurs when the vehicle enters the span but the maximum acceleration of beam 6 occurs when the vehicle is at midspan or leaving the bridge.

Current bridge specifications attempt to control vibrations by limiting the maximum live load deflection, which may unjustly penalize designs that use more flexible, high-strength steel beams. Figure 3 shows the variation of maximum midspan accelerations as beam stiffness is reduced. The basic design uses five W36×230 A36 steel beams. Equal strength can be provided by five W36×182 A572-50 beams. Although the maximum acceleration increases somewhat as stiffness is reduced, the relation is certainly less severe than an inverse proportion.

Vehicle Parameters

It is well known that vehicle speed has a strong influence on bridge vibrations. In Figure 4 maximum midspan accelerations for a five-beam bridge are plotted versus vehicle speed. Bridge accelerations are almost directly proportional to vehicle speed over the indicated speed range.

The effect of the transverse position of the vehicle on a five-beam, 18-m (60-ft) span bridge was studied by determining the maximum midspan accelerations for six cases. Results indicate that the accelerations of the edge beams are greatest when the vehicle travels along the edge of the roadway and tend to decrease when the vehicle travels near the centerline of the bridge. In contrast, center-beam accelerations increase as the vehicle moves toward the centerline and are slightly larger than edge-beam accelerations when the vehicle straddles the centerline. In most practical situations, however, edge-beam accelerations are larger than those of the interior beams.

Surface Roughness

Several test reports (11, 12, 13) have indicated that surface roughness is a very significant factor affecting the vibration of highway bridges. These reports have recommended that the bridge surface should be as smooth as possible. For all of the results previously reported here, the bridge surface was assumed to be smooth.

Surface roughness is assumed to be represented by

Figure 1. Maximum midspan accelerations for simple-span steel beam bridges.

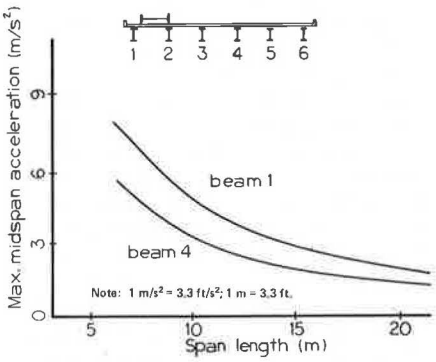

Figure 2. Acceleration history curves.

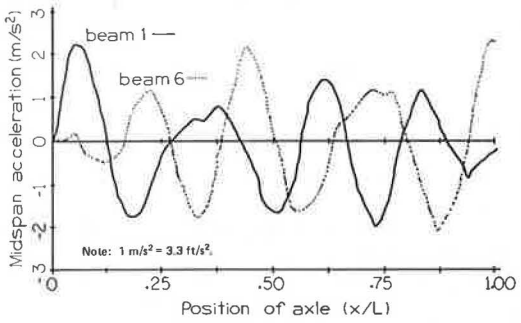

Figure 3. Acceleration versus beam stiffness for simple-span bridge.

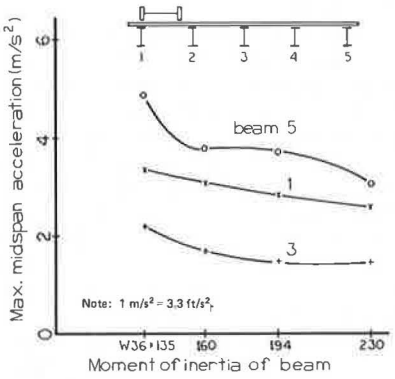

Figure 4. Acceleration versus vehicle speed for simple-span bridge.

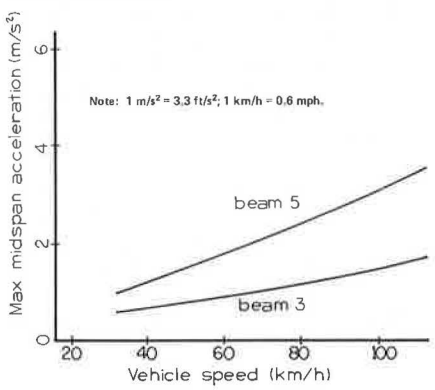

some number of half sine waves passing through the supports. Both the number of half sine waves and the amplitude can be varied. It is assumed that the shape and the amplitude of bridge surface roughness are the same under both wheels of the vehicle.

Figure 5 shows the results of determining the maximum midspan accelerations for 0 to 19 half sine waves of 13-mm (0.5-in) amplitude roadway roughness. Again, a 32 667-kg (72 000-lb) vehicle traveled at 96 km/h (60 mph) near the edge of the roadway on a five-girder, 18-m (60-ft) span bridge. It is evident that the accelerations are not influenced by up to 3 half sine waves of roughness; however, the effect increases markedly when the number of half waves exceeds 5 and reaches its peak when the surface roughness consists of 12 half sine waves. For the two peaks at 7 and 12 half sine waves, the times required for the vehicle to cross a single roughness wave correspond fairly closely to the first two natural frequencies of the bridge. The maximum accelerations for a rough roadway surface are as much as five times those for the same bridge with a smooth deck. Of course, the probability of a perfectly periodic deck roughness is rather small for a real bridge. But the significance of the effect is obvious. For the nearly resonant condition, maximum accelerations are approximately proportional to the amplitude of the surface roughness.

CONTINUOUS-BEAM BRIDGES

Method of Analysis

A general theory for the analysis of continuous bridges was developed by Huang and Veletsos (14). The computer program used in this study, which was developed by Huang (4), was previously used by Nieto-Ramirez and Veletsos (15) in an extensive study of the dynamic response of three-span bridges. Application of the program here is limited to two- and three-span symmetric beam bridges.

In this analysis the bridge is idealized as a single, continuous beam and the resulting system, which has an infinite number of degrees of freedom, is replaced by a discrete system with a finite number of degrees of freedom by replacing the distributed mass by a series of concentrated point masses and considering the beam stiffness to be distributed as in the original structure. Bridge damping is assumed to be of the absolute viscous type and is approximated by dashpots located at mass coordinate points. The analysis is based on ordinary beam theory and neglects the effects of shearing deformation and rotary inertia.

Because the bridge has been idealized in this analysis as a single beam, the rolling effect of the vehicle cannot be considered. Even when it is treated as a plane system, however, a vehicle is a complex mechanical system. In this analysis a tractor-trailer vehicle is represented by a three-axle load unit that consists of two interconnected masses (Figure 6). Each axle is represented by two springs in series and a frictional mechanism that simulates the effect of friction in the suspension system. The second spring is active only when the axle force exceeds the limiting friction value. Viscous damping is neglected.

Writing the equations of motion for the vehicle and the concentrated masses of the bridge yields a set of simultaneous, second-order differential equations, equal in number to the number of degrees of freedom of the bridge-vehicle system. These equations are solved by a numerical integration scheme in which the evaluation of the interacting forces between the bridge and the vehicle is a major intermediate step. As the integration of the differential equations is carried out, the values of all coordinates, accelerations, and interacting forces are determined. Values of corresponding deflections and moments at any section can then be determined by statics.

Acceleration Studies

Both two- and three-span symmetric, continuous-girder bridges have been studied extensively (16); because the results are similar, only two-span bridges will be discussed here. Bridge data are again those of the U.S. Bureau of Public Roads (10), and the study is restricted to steel continuous-beam bridges with reinforced concrete decks. Unless stated otherwise, the roadway surface is assumed to be smooth.

The accuracy of the analysis now depends on the number of lumped masses chosen as well as the number of integration steps. Good stability of the solution was obtained by dividing the time required for the vehicle to cross the bridge into 2000 integration steps. The bridge was modeled by lumping the masses at the quarter and midpoints of each span, as suggested by Huang (4).

Bridge Parameters

Figure 7 shows the maximum nodal accelerations for three standard-design bridge spans. The roadway width is 13 m (44 ft) and the 190-mm (7.5-in) slab is supported by six rolled steel beams. Bridge damping is taken as 2 percent of critical damping. The vehicle is an HS20 three-axle truck moving at a speed of 96 km/h (60 mph). As in the case of simple-span bridges, higher accelerations occur on the shorter spans. Maximum accelerations for two-span bridges were found to be about 1.5 times larger than those for three-span bridges of equal span length. Highest accelerations occur in the simple-span bridges.

The effect of varying girder stiffness was investigated for a bridge with two 18-m (60-ft) spans. Although the results shown in Figure 8 are somewhat irregular, maximum accelerations for that bridge would not be significantly increased by replacing the A36 beams with smaller, high-strength steel beams. The important point here is, of course, that deflection control is not directly related to vibration control.

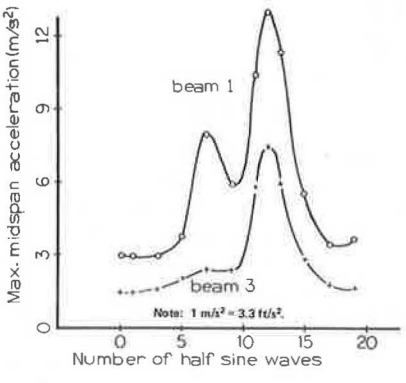

Figure 5. Acceleration versus roadway roughness for simple-span bridge.

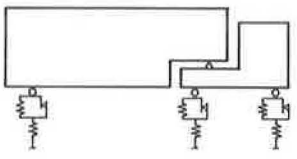

Figure 6. Three-axle vehicle model.

Figure 7. Maximum accelerations for two-span steel-beam bridges.

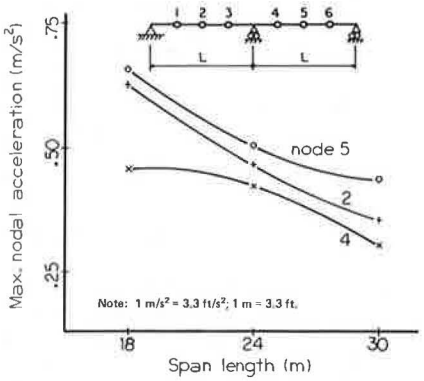

Figure 8. Acceleration versus beam stiffness for two-span bridge.

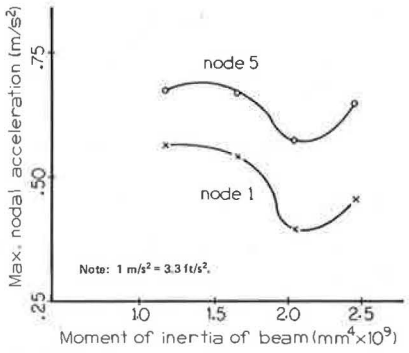

Figure 9. Acceleration versus axle spacing for two-span bridge.

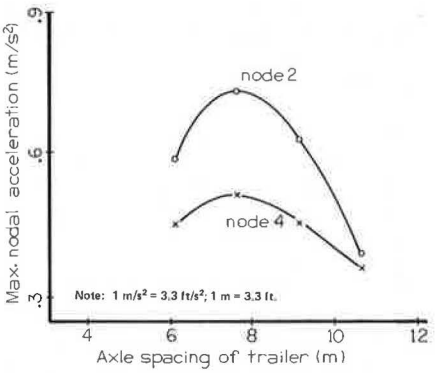

Figure 10. Effect of initially oscillating vehicle on bridge acceleration.

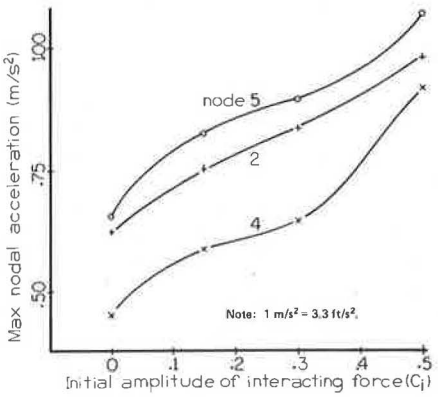

Figure 11. Acceleration versus roadway roughness for two-span bridge.

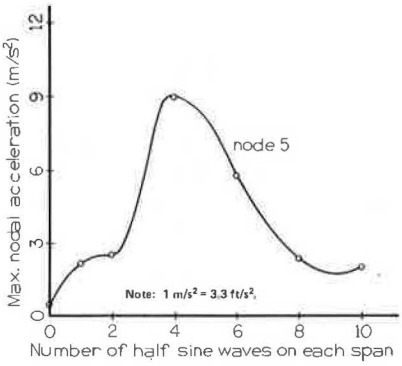

Vehicle Parameters

The values for the geometric, mass, and suspension parameters of the vehicle model were chosen to make the model closely represent a typical, heavily loaded tractor-trailer. The spacing of the tractor axles, although taken to be 3.7 m (12 ft), might be considered variable. As shown in Figure 9, the maximum acceleration for two 18-m (60-ft) spans occurs when the trailer axle spacing is about 8 m (25 ft) or 0.42 times the span length. The critical axle spacing ratio for three-span bridges is 0.37 to 0.43.

A comparison of maximum accelerations was also made by using one-, two-, and three-axle vehicle models. Maximum accelerations were about the same for two- and three-axle vehicle models, but they were about two-thirds of the magnitudes produced by the single-axle model. As in the case of simple-span bridges, a marked increase in acceleration with vehicle speed was found.

Maximum accelerations were also computed for different values of frequency ratio (the ratio of the natural frequency of the vehicle on its tires to the natural frequency of the bridge). Generally, the magnitudes of accelerations at the nodes were about the same for all values of frequency ratio although the midspan accelerations were slightly higher when the vehicle and the bridge had the same natural frequency.

A real vehicle is likely to be oscillating somewhat as it enters a bridge because of irregularities in the approach pavement and a possible discontinuity at the abutment. The most significant parameter for representing initial oscillations is the initial-axle-force variation (C_i). The initial axle force is equal to $(1 + C_i)$ times the static force. Figure 10 shows maximum nodal accelerations for four values of C_i. The same C_i value is assumed for each axle. According to Nieto-Ramirez and Veletsos (15), $C_i = 0.15$ might correspond to a 3-mm (0.125-in) pavement irregularity and $C_i = 0.50$ might represent a large discontinuity at the abutment. It can be seen that the initial oscillation causes a 30 to 50 percent increase in maximum acceleration for this bridge-vehicle system, which is assumed to have a smooth deck surface. An investigation that considered a phase angle difference between initial oscillations of the trailer axles found that maximum accelerations varied less than 20 percent.

Surface Roughness

All of these two-span studies assumed a smooth bridge-deck surface. The effect of surface roughness has been investigated for a standard design bridge with two 18-m (60-ft) spans that was loaded by an HS20 truck. The deck surface was represented by an integral number of half sine waves. The influence of roadway roughness is shown in Figure 11. With four half waves of roughness in each span, the frequency of oscillation of the interacting forces is close to the fundamental natural frequency of the bridge and the nearly resonant response occurs. Thus, for both simple and continuous bridges,

surface roughness seems to be the most significant factor affecting roadway accelerations.

CONCLUSIONS

Analytical studies have shown that the significant parameters that influence bridge accelerations are vehicle speed and weight, bridge-span length, and surface roughness. Maximum acceleration levels were found to be rather high for typical simple-span bridges; however, accelerations for two- and three-span continuous bridges exceeded the suggested comfort limit only when severe effects of surface roughness were included.

Current specifications attempt to control bridge vibrations by limiting girder flexibility. In this study, only a small increase in maximum acceleration resulted when girder flexibility was increased by replacing A36 beams with smaller, high-strength steel beams. Thus, using more efficient, high-strength steel designs may be possible without adversely affecting user comfort.

ACKNOWLEDGMENTS

The aid of W. H. Walker of the Civil Engineering Department of the University of Illinois in making available the computer programs used in this study is gratefully acknowledged. This analytical study is a part of the Joint Highway Research Project, Bridge Vibration Studies, which involves the cooperative efforts of the School of Civil Engineering of Purdue University and the Indiana State Highway Commission. The research is being carried out under the sponsorship of the Federal Highway Administration, U.S. Department of Transportation.

REFERENCES

1. Standard Specifications for Highway Bridges. AASHO, 11th Ed., 1973.
2. C. Oran and A. S. Veletsos. Analysis of Static and Dynamic Response of Simple-Span, Multigirder Highway Bridges. Univ. of Illinois, Urbana, Civil Engineering Studies, Structural Research Series 221, July 1961.
3. A. S. Veletsos and T. Huang. Analysis of Dynamic Response of Highway Bridges. Journal of Engineering Mechanics Division, Proc., ASCE, Vol. 96, No. EM5, Oct. 1970.
4. T. Huang. Dynamic Response of Three Span Continuous Highway Bridges. Univ. of Illinois, Urbana, PhD thesis, 1960.
5. R. N. Wright and W. H. Walker. Vibration and Deflection of Steel Bridges. Engineering Journal, American Institute of Steel Construction, Vol. 9, No. 1, Jan. 1972.
6. D. T. Wright and R. Green. Human Sensitivity to Vibration. Department of Civil Engineering, Queen's Univ., Kingston, Ontario, Rept. 7, Feb. 1959.
7. K. H. Lenzen. Vibration of Steel Joist-Concrete Slab Floors. Engineering Journal, American Institute of Steel Construction, July 1966.
8. R. N. Janeway. Vehicle Vibration Limits to Fit the Passenger. National Passenger Car and Production Meeting, SAE, Detroit, 1948.
9. J. F. Wiss and R. A. Parmalee. Human Perception of Transient Vibrations. Journal of Structural Division, Proc., ASCE, Vol. 100, April 1974, pp. 773-787.
10. Standard Plans for Highway Bridge Superstructures. Bureau of Public Roads, U.S. Department of Commerce, 1968.
11. L. T. Oehler. Vibration Susceptibilities of Various Highway Bridge Types. Journal of Structural Division, Proc., ASCE, Paper 1318, July 1957.
12. Dynamic Studies of Bridges on the AASHO Road Test. HRB, Special Rept. 71, 1962.
13. D. T. Wright and R. Green. Highway Bridge Vibrations—Part II. Ontario Joint Highway Research Project, Rept. 5, May 1964.
14. T. Huang and A. S. Veletsos. Dynamic Response of Three Span Continuous Bridges. Univ. of Illinois, Urbana, Civil Engineering Studies, Structural Research Series 190, 1960.
15. J. A. Nieto-Ramirez and A. S. Veletsos. Response of Three-Span Continuous Highway Bridges to Moving Vehicles. Univ. of Illinois, Urbana, Civil Engineering Studies, Structural Research Series 278, Jan. 1964.
16. T. Aramraks. Highway Bridge Vibration Studies. Purdue Univ., West Lafayette, Ind., PhD thesis, 1975.

Publication of this paper sponsored by Committee on Dynamics and Field Testing of Bridges.

Abridgment

Load Distribution on a Timber-Deck and Steel-Girder Bridge

Marvin H. Hilton, Virginia Highway and Transportation Research Council, Charlottesville
L. L. Ichter, David W. Taylor Naval Ship Research and Development Center, Washington, D.C.

Some general studies, as well as investigations of load distribution, have been conducted on timber bridges (1, 2, 3, 4). Most of this research has concerned structures with timber decks and timber girders. A laboratory study conducted by Agg and Nichols (5) was concerned with wood floors on steel floor joists. The study re-

Figure 1. Floor plank fasteners.

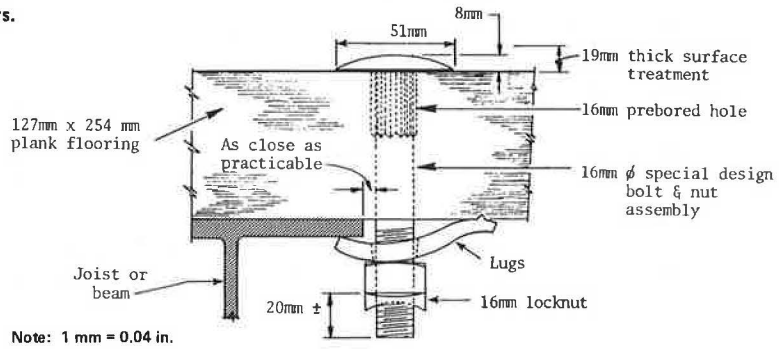

Figure 2. Floor fastener arrangement.

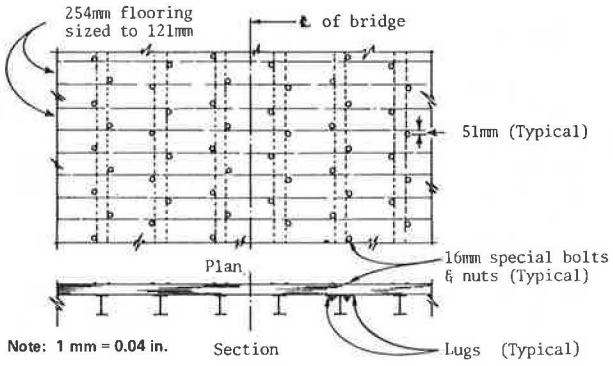

ported here deals with the load distribution on an in-service bridge with a timber deck and steel girders.

DESCRIPTION OF TEST STRUCTURE

The test bridge was a 7-m (23-ft) wide by 14.8-m (48.5-ft) long simple-span structure that conforms to the Virginia standards for wooden floor-steel beam bridges designed for H20 loading. Figure 1 shows the standard fasteners with which the nominal 127 × 254-mm (5 × 10-in) floor planks are attached to the steel girders. The fastener bolts are inserted through predrilled holes in the planks and locked to the upper flange of each girder in the staggered arrangement shown in Figure 2. The deck floor is covered with a 19-mm (0.75-in) bituminous wearing surface.

The superstructure of the bridge is composed of 14 21WF68 steel beams spaced 0.5 m (19.75 in) apart on centers for the interior bays and 0.6 m (24 in) apart on centers for the first two exterior bays on each side of the span. Only 6 of the 14 girders are anchored to the abutment seats; all others simply rest on the abutment beam seats.

INSTRUMENTATION AND LOADING

Strain gauges were applied to 8 of the 14 girders at midspan. The structure was loaded with a truck that simulated the type 3 loading designated by the American Association of State Highway and Transportation Officials (AASHTO) (6). The type 3 loading has a total weight of 20.9 Mg (23 tons); the truck used in this study weighed 20.6 Mg (22.7 tons). The distance between the front and the first rear axles of the truck, however, was 0.51 m (1.67 ft) shorter than the 4.57 m (15 ft) designated for the type 3 load. Thus, for the span investigated, the loading used produced midspan moments in the girders that were very close to those that would be developed by the type 3 legal load unit: 290 032 N·m (213 347 lbf·ft) actually applied versus 285 174 N·m (209 774 lbf·ft) for type 3. It should be noted that the type 3 loading, unlike other types of legal loadings, will develop the maximum moment in a 14.8-m (48.5-ft) bridge span.

The study determined the stresses in the steel girders that resulted from various loading sequences. Load distribution characteristics of the structure were determined under varying conditions with loosened floor fasteners. More details on the instrumentation, the type of loading, and the test procedures are available in another report (7).

RESULTS

If all of the live load moment developed by the line of the wheels of the test vehicle were carried by a single girder with no lateral load distribution, a stress of 126.5 MPa (18 350 lbf/in^2) would be developed in that member. Considerable lateral load distribution takes place, of course, and it was found that the highest stresses developed on the interior girders of the bridge were on the order of 41.4 MPa (6000 lbf/in^2) or less. The highest stress developed for all of the lateral axle positions used on the span was 49.8 MPa (7220 lbf/in^2); this occurred at an exterior beam when the fasteners on the four adjacent girders were loosened and the tread of the nearest tire was 51 mm (2 in) from the curb. In this case the resultant of the load (placed on the bridge by the two wheels of one side of a rear axle) would fall midway between the exterior and the first interior girders, which are spaced 0.6 m (2 ft) apart.

Figure 3 shows the midspan stresses on the lower flanges of the steel girders for conditions in which floor fasteners were tightened and loosened. These data show the following results.

1. The live load stresses resulting from the truck loadings are laterally distributed in a reasonably consistent manner, even when the fasteners are loosened.
2. The live load stresses in the steel girders are reasonably low. Although design stresses must include dead load and impact, the maximum stress recorded on the interior girders was only 31 percent of the 138 MPa (20 000 lbf/in^2) allowable for A36 steel. In most instances the maximum stresses recorded for the interior girders were on the order of 25 to 30 percent of the allowable total.
3. Loosening of the deck plank fasteners does not have a very significant effect on either the magnitude or the lateral distribution of the stresses.

LOAD DISTRIBUTION FACTORS

The current practice of the Virginia Department of Highways and Transportation is to distribute the live load

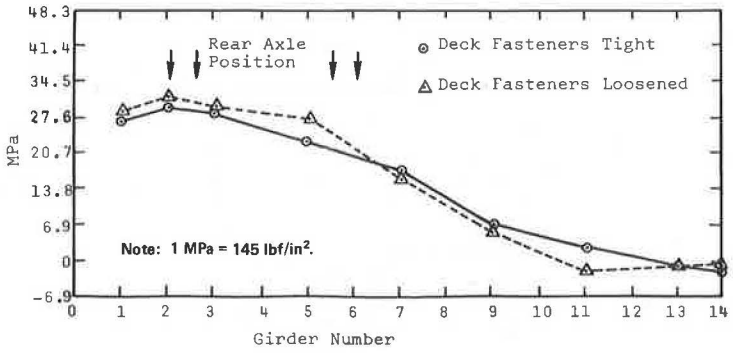

Figure 3. Lateral midspan stress distribution produced by truck loading position shown for conditions of loosened and tightened fasteners.

moments to the interior girders of all timber-deck bridges by using a factor of S/4, where S is the spacing in feet between adjacent girders specified by AASHO (8) (because the AASHO values for load distribution are empirically derived in customary units, no SI equivalents are given). The live load is distributed to the exterior girders by using the reaction of the wheel load obtained by assuming the flooring to act as a simple beam between the exterior and the first interior girders.

Load Distribution to Interior Girders

The load distribution factor of S/4 was found to be conservative in all cases for the interior girders. The highest load distribution to interior girders was developed by loading both lanes of the two-lane bridge. The highest load distribution factor obtained from the data would yield an equivalent formula of S/5.12. Considering the remaining lower stresses obtained in the investigation, the denominator of the formula would be larger. These data suggest that, for 127-mm (5-in) thick timber-deck bridges such as the SS-4 Virginia standard structure investigated, a distribution factor for the interior girders of S/5 would be adequate for legal limits.

Load Distribution to Exterior Girders

The load distribution factor determined for the exterior girders by proportioning the load as the reaction of a simple beam between the exterior and the first interior girders was found to be inadequate in some instances. Specifically, the Virginia procedure used to evaluate the exterior girders calls for positioning the resultant of the wheel line 0.55 m (18 in) from the curb, which corresponds to the study loading position in which the nearest tire tread is 191 mm (7.5 in) from the curb. By using the simple-beam assumption, a distribution factor of 191/609 (7.5/24), or 0.315, would be obtained. Moving the loading position from 191 to 51 mm (7.5 to 2 in) from the curb changes the calculated simple-beam distribution factor from 0.315 to 0.50 and the actual factor from 0.343 to 0.39. Thus, for the 140-mm (5.5-in) lateral change of wheel-load position, the actual change in load distribution was much less than that calculated by the procedure for simple-beam reaction. Because the 0.343 and 0.39 factors can be transformed respectively to S/5.38 and S/5.08, a general distribution factor of S/5 could be used. An analysis of other loading positions in the area between the first and second girders suggests that the use of a distribution factor of S/5 would be more realistic than the current procedure used for exterior girders.

ACKNOWLEDGMENTS

We thank district bridge engineers W. Schwartz and R. Booth of the Virginia Department of Highways and Transportation for their assistance in selecting and testing the bridge. The project was financed by the Virginia Department of Highways and Transportation and was under the general supervision of J. H. Dillard, Head, Virginia Highway and Transportation Research Council.

The opinions, findings, and conclusions expressed in this paper are ours and not necessarily those of the sponsoring agencies.

REFERENCES

1. G. P. Boomsliter, C. H. Cather, and D. T. Worrell. Distribution of Wheel Loads on a Timber Bridge Floor. West Virginia Univ., Bulletin 24, May 1951.
2. W. C. Huntington, W. A. Oliver, M. W. Jackson, and W. T. Cox. The Distribution of Concentrated Loads by Laminated Timber Slabs. Univ. of Illinois, Bulletin 424, April 1954.
3. E. C. O. Erickson and K. M. Romstad. Distribution of Wheel Loads on Timber Bridges. U.S. Forest Products Laboratory, Research Paper FPL44, Dec. 1965.
4. P. Zia, W. T. Wilson, and W. H. Rowan. A Study of Load Distribution Characteristics of Single and Double Layer Timber Bridge Decks Supported by Multiple Stringers. North Carolina State Univ., June 1964.
5. T. R. Agg and C. S. Nichols. Load Concentrations on Steel Floor Joists of Wood Floor Highway Bridges. Iowa Engineering Experiment Station, Ames, Bulletin 53, April 1919.
6. Manual for Maintenance Inspection of Bridges. AASHTO, 1974.
7. M. H. Hilton and L. L. Ichter. An Investigation of the Load Distribution on a Timber Deck-Steel Girder Bridge. Virginia Highway and Transportation Research Council, Rept. 76-R30, Dec. 1975.
8. Standard Specifications for Highway Bridges. AASHO, 11th Ed., 1973.

Publication of this paper sponsored by Committee on Dynamics and Field Testing of Bridges.

Abridgment

Dynamic Properties of Beam-Slab Highway Bridges

Celal N. Kostem, Lehigh University

Determination of the dynamic response of bridges has been of interest and concern to engineers for more than three-quarters of a century (4) primarily because of the need to define the amplification of the static response of bridges caused by moving vehicles. This has traditionally been accomplished by oversimplifying the bridge superstructure into an equivalent beam and thus ignoring the high internal indeterminacy of the superstructure. Equivalent-beam modeling encouraged the use of the impact factor or the dynamic load factor in obtaining dynamic response.

Refined analytical studies on simple-span beam-slab highway bridges with prestressed concrete I-beams and without skew have indicated that the true dynamic behavior of the bridge superstructure can be simulated by finite-element modeling of the total superstructure (3). The studies have also indicated that one of the major benchmarks in the differentiation of the dynamic responses of various bridges is the correct determination and comparison of the predominant natural periods of vibration of the superstructure (3, 4). Full-scale field studies carried out on a limited number of bridges have resulted in experimental determination of the first natural period of vibration of bridge superstructures (5). Bridge engineers have been able to make only limited use of the test results because of the limited variation in the major design dimensions of the field-tested bridges: Another bridge with different design dimensions could have a substantially different period of vibration. Before the start of the parametric study reported here, the natural vibration periods obtained in field test were recomputed by means of the finite-element method, and good correlation was observed (3).

DESIGN AND ANALYSIS OF BRIDGES

Eighteen simple-span beam-slab bridges with prestressed concrete I-beams and without skew were designed to represent bridges of this type encountered in the field (6). The design dimensions of the test bridges are given in Table 1. The beams used in the design process correspond to the standard beams used in the state of Pennsylvania. Table 2 gives the stiffness properties of the beams. Although the study used only 18 bridges, previous investigations (2) have indicated that this is a sufficient number if the sample structures are carefully chosen so that they closely approximate the dimensions of existing bridges. The results presented here can be applied to bridges of other dimensions through interpolation and engineering judgment (2).

In defining the dynamic characteristics of the bridges, the superstructures were simulated by using the finite-element method. The bridge superstructure was considered an assemblage of plate bending and beam elements. The analysis was performed by using the SAP IV program (1). Only the first three natural periods of vibration of the superstructures are presented here, partly because of space limitations but also because three periods are sufficient to illustrate the dynamic properties of the bridges. It should be noted that the periods reported here are the natural periods of the bridge; that is, no vehicle is assumed to be on the bridge. The periods of bridges loaded with vehicles will not, however, be substantially different from those given here. The vibrating mass of vehicles is small compared to the mass of the bridge superstructure. These periods can thus be used with good reliability to approximate loaded periods for long-span bridges and with decreasing reliability as span lengths get shorter.

RESULTS

Natural periods of vibration for the three predominant mode shapes are given (in seconds) below. In this and the following table, T_1, T_2, and T_3 denote the first, second, and third natural periods respectively.

	Period (s)		
Bridge	T_1	T_2	T_3
1	0.066	0.059	0.048
2	0.077	0.064	0.052
3	0.075	0.069	0.063
4	0.082	0.073	0.063
5	0.075	0.068	0.064
6	0.082	0.077	0.070
7	0.134	0.114	0.076
8	0.109	0.095	0.071
9	0.136	0.126	0.106
10	0.116	0.106	0.093
11	0.138	0.132	0.120
12	0.120	0.114	0.105
13	0.181	0.157	0.098
14	0.160	0.139	0.095
15	0.177	0.166	0.140
16	0.165	0.152	0.131
17	0.180	0.172	0.158
18	0.168	0.159	0.145

Although there is a substantial change in the design dimensions of the bridges, the variation in the first natural period of the bridge superstructures is not highly sensitive to the major changes in the design dimensions. For a given span length, the first natural period of vibration tends to remain relatively constant. It can thus be concluded that the first mode of vibration and the corresponding period are primarily a function of the span length of the bridge superstructure.

The equivalent-beam approach uses the following formula to predict the natural periods of vibration of the bridge superstructure:

$$T_i = (2\pi/A_i)\sqrt{ML^4/EI} \qquad (1)$$

where

M = beam mass per unit length,
L = beam length,
E = beam modulus of elasticity, and
I = beam moment of inertia.

The coefficient A_i is used to obtain different natural periods (4). The values for the first three periods are A_1 = 9.87, A_2 = 39.5, and A_3 = 88.9.

In using the equivalent-beam approach for beam-slab bridges, it is assumed that the beams are the predominant load-carrying system. In computing mass and inertia properties, only the beams are considered. Using

Table 1. Design dimensions of test bridges.

Bridge	Span (m)	Width (m)	Slab Thickness (mm)	Beam Spacing (m)	Number of Beams	Beam
1	12.20	7.93	190	1.46	6	I
2	12.20	8.46	203	2.44	4	I
3	12.20	13.57	190	1.60	9	I
4	12.20	14.02	215	2.56	6	I
5	12.20	19.05	190	1.66	12	I
6	12.20	19.51	215	2.61	8	I
7	19.82	7.93	190	1.46	6	II
8	19.82	8.38	203	2.44	4	IV
9	19.82	13.41	190	1.60	9	III
10	19.82	13.95	215	2.56	6	IV
11	19.82	18.90	190	1.66	12	III
12	19.82	19.44	215	2.61	8	IV
13	27.44	7.77	190	1.46	6	V
14	27.44	8.38	203	2.44	4	VII
15	27.44	13.41	190	1.60	9	VI
16	27.44	13.87	203	2.56	6	VII
17	27.44	18.90	190	1.66	12	VI
18	27.44	19.36	203	2.61	8	VII

Note: 1 m = 3.28 ft; 1 mm = 0.0394 in.

Table 2. Stiffness properties of beams.

Beam	Maximum Moment of Inertia (mm^4)	Minimum Moment of Inertia (mm^4)	Area (mm^2)	St. Venant Torsional Stiffness (mm^4)	Notation[a]
I	13.66 (10^9)	2.66 (10^9)	234 (10^3)	3.81 (10^9)	PDT20/30
II	31.66 (10^9)	7.74 (10^9)	397 (10^3)	13.35 (10^9)	PDT24/36
III	34.69 (10^9)	10.36 (10^9)	443 (10^3)	17.65 (10^9)	PDT26/36
IV	71.96 (10^9)	8.37 (10^9)	457 (10^3)	13.04 (10^9)	PDT24/48
V	88.50 (10^9)	8.98 (10^9)	492 (10^3)	14.64 (10^9)	PDT24/51
VI	106.33 (10^9)	9.59 (10^9)	526 (10^3)	16.52 (10^9)	PDT24/54
VII	195.87 (10^9)	15.87 (10^9)	675 (10^3)	23.00 (10^9)	PDT26/63

Note: 1 mm^4 = 2.4 (10^{-6}) in^4; 1 mm^2 = 0.0015 in^2

[a] From Standards for Bridge Design of Pennsylvania Department of Transportation (6).

this concept and the formula given above yields the natural periods given in the table below.

Bridge	Period (s) T_1	T_2	T_3
1	0.163	0.041	0.018
2	0.194	0.049	0.022
3	0.167	0.042	0.019
4	0.202	0.051	0.023
5	0.169	0.042	0.019
6	0.203	0.051	0.023
7	0.337	0.087	0.038
8	0.256	0.064	0.029
9	0.326	0.082	0.037
10	0.263	0.066	0.030
11	0.329	0.082	0.037
12	0.507	0.127	0.057
13	0.398	0.099	0.045
14	0.329	0.083	0.037
15	0.377	0.094	0.042
16	0.333	0.083	0.037
17	0.379	0.095	0.043
18	0.334	0.084	0.037

A comparison of the data in the preceding table, for true periods, and those in the table above, for approximate periods, indicates that substantial discrepancies exist in all values. It can thus be stated that the equivalent beam defined by the above approach will yield incorrect results.

Another approach used to define equivalent-beam properties has been to consider the full slab and the beams in the definition of the appropriate values. This corresponds to the assumption that bridge beams will essentially act like T-beams, the slab width being the spacing of the beams. The use of Equation 1 for this assumption results in a first period of vibration that is close to the true periods; however, unacceptable differences still exist in the higher natural periods. Thus, if it is necessary to find the first period of vibration of the beam-slab bridge superstructure, fully acceptable results can be obtained by using the equivalent-beam approach and the appropriate formula and assuming that both the beams and the bridge deck will fully participate through their contributions to stiffness and mass.

CONCLUSIONS

The dynamic or vibrational characteristics of beam-slab bridge superstructures can be predicted and compared by use of predominant natural periods of vibration. The parametric study indicated that

1. The first natural period of bridges is predominantly dependent on the span length,
2. The dynamic characteristics of bridges vary as bridge configurations change,
3. The first natural period of bridges, regardless of the bridge configuration, does not vary substantially for a given span length,
4. The use of the equivalent-beam approach with the correct formula and the correct stiffness and mass contributions results in an accurate estimate of the first natural period of vibration of the structure but in poor estimates for all other dynamic properties of the structure, and
5. The contribution of the slab should be included in the estimation of the dynamic characteristics of bridge superstructures.

REFERENCES

1. K. J. Bathe, E. L. Wilson, and F. E. Peterson. SAP IV—A Structural Analysis Program for Static and Dynamic Response of Linear Systems. Earthquake Engineering Research Center, Univ. of California, Berkeley, Rept. EERC 73-11, June 1973 (revised April 1974).
2. E. S. DeCastro and C. N. Kostem. Load Distribution in Skewed Beam-Slab Highway Bridges. Lehigh Univ., Bethlehem, Penn., Fritz Engineering Laboratory Rept. 378A.7, Dec. 1975.
3. W. S. Peterson and C. N. Kostem. Dynamic Analysis of Beam-Slab Highway Bridges. HRB, Highway Research Record 428, 1973, pp. 57-63.
4. S. Timoshenko. Vibration Problems in Engineering. Van Nostrand, New York, 1928.
5. M. A. Zellin, C. N. Kostem, and D. A. VanHorn. Structural Behavior of Beam-Slab Highway Bridges: A Summary of Completed Research and Bibliography. Lehigh Univ., Bethlehem, Penn., Fritz Engineering Laboratory Rept. 387.1, May 1973.
6. Standards for Bridge Design (Prestressed Concrete Structures). Bureau of Design, Pennsylvania Department of Transportation, Harrisburg, BD-201, March 1973.

Publication of this paper sponsored by Committee on Dynamics and Field Testing of Bridges.

Portable Recorder for Bridge Stresses

Mark W. Williams, Norton and Schmidt Consulting Engineers, Kansas City, Missouri
James W. Baldwin, Jr., Department of Civil Engineering, University of Missouri—Columbia

Development and operation of a portable instrument for recording strain events in bridges under field-service conditions are described. The instrument consists of a transducer, which is clamped to the flange of a bridge by four allen screws; a set of mechanical counters driven by electronic logic circuitry; a battery pack; and a tamper-proof enclosure. As much as 80 d of continuous operation can be realized before batteries must be serviced. Each counter is incremented every time the strain reaches the triggering level selected for that counter. Triggering levels are selected to be distributed over a range slightly greater than the strain range expected in the bridge. For the usual case, in which the triggering levels are all in the elastic range, a simple hand calculation will produce a stress histogram from the counter readings. The theory and a procedure for predicting bridge life from the collected data are also presented. Results of a short field test indicate that the instrument provides a practical and economical means by which relatively unskilled personnel can collect stress-history data.

In recent years, limited field studies (1, 2, 3, 4, 5, 6, 7, 8, 9, 10) have indicated that actual service stresses in highway bridges may be far below the calculated maximum stresses for which bridges are designed; many more data are needed, however, before conclusions can be drawn as to whether present design criteria can or should be revised.

Field studies of service stresses now require a substantial amount of expensive equipment and skilled research personnel. Unfortunately, these studies have been limited, by expense, to observations of a relatively small number of bridges for relatively short periods of time. Clearly, there is a need for a more economical means of data collection that will allow studies to be performed on a much wider variety of bridges for much longer periods of time.

Availability of the instrument described in this paper will make it possible for highway department personnel to collect and interpret, on the spot, load-history information from a variety of bridges at a relatively low cost. In addition to determining the actual service stresses in bridges, the instrument could also be used to observe (a) the long-range trends of traffic volume, (b) the effectiveness of weigh stations, (c) the effects of changes in legal weight limits, and (d) the presence of overweight vehicles in areas where there are no weigh stations or at times when such stations are closed.

THEORY OF OPERATION

Fatigue Considerations

Most recent load-history studies have incorporated a fatigue analysis based on collected data, which requires knowledge about the behavior of the particular material under fatigue loading and the important parameters that govern this behavior. Fisher and others (13) conducted in-depth studies on fatigue with respect to weldments on steel beams and concluded that stress range alone is the dominant variable in fatigue analyses of structural steel bridges. Fatigue curves for a variety of structural details have been developed from the accumulated data. These curves are represented by a linear log-log relation between the stress range (Sr) and the cycles to failure (N). The stress range, as defined by Fisher and others (13), Douglas (5), and Munse and Stallmeyer (12), is taken as the algebraic difference between the maximum and minimum stress values from each loading cycle. A typical stress or strain trace is shown in Figure 1.

Construction of Histogram

Load histories are generally collected as an analog recording that is subsequently processed through an analog-to-digital converter. Then the maximum and minimum stress values are determined from the digital record and are combined to obtain the stress range. The data are subsequently grouped in discrete intervals from which the frequency of occurrence of stress ranges within each interval may be determined. The result of this procedure, represented graphically, is known as the stress-range-frequency histogram (5). Figure 2 shows an example of such a histogram.

Assume that a series of counters is introduced in place of the sophisticated system of data acquisition. Each counter is incremented when the stress level reaches a preselected value, as shown in Figure 3. A given counter cannot be incremented again until the stress level has gone below some preselected value near zero. For the single cycle shown, counters 1 to 4 are each incremented once. Counters 5 and 6 are not incremented because the analog signal representing the strain trace does not exceed their corresponding stress level.

If it is assumed that a similar sequence of counting occurs for each trace caused by a passing vehicle, then, for the length of the test period associated with a particular bridge study, each counter total (C_i) reflects the number of times that its associated stress level (σ_i) was exceeded. Furthermore, if no negative portion of the strain trace exists, as in Figure 3, then the maximum value of σ in any trace is also the stress range for that trace. If Sr_i is defined as the stress range equal to σ_i and Cr_i is the number of times Sr_i has been exceeded, then

$$Cr_i = C_i \qquad i = 1, 2, \ldots, m \tag{1}$$

where m is the number of active counters. If the highest triggering level (σ_m) is high enough that it is never exceeded,

$$Cr_m = C_m = 0 \tag{2}$$

and Cr_{m-1} is the number of occurrences of stress ranges between the values of Sr_{m-1} and Sr_m. In general, $Cr_i - Cr_{i-1}$ is the number of occurrences of stress ranges between the values of Sr_{i-1} and Sr_i. The stress-range histogram can thus be constructed directly from counter differences. Clearly, C_1 is equal to the total number of significant events that occurred over the test period.

Consider now that a negative portion of the strain trace does occur, which it would in a multispan bridge structure. Figure 4 shows a simulation of a typical loading cycle in which each counter associated with a negative stress level is incremented in the manner previously indicated for positive counters. The stress levels (Figure 4) must then be combined by some method in order to obtain the necessary stress ranges for subsequent analyses.

The stress range for the trace shown in Figure 4 just exceeds σ_3 to σ_5. In general, it can be assumed that stress events that produce relatively large positive peaks also produce relatively large negative peaks. Then the stress levels shown in Figure 4 may be associated to form stress ranges by a comparative analysis of the cumulative number of exceedences (C_i) and (C_j) of positive and negative stress levels (σ_i) and (σ_j) respectively.

Figure 1. Typical stress or strain trace.

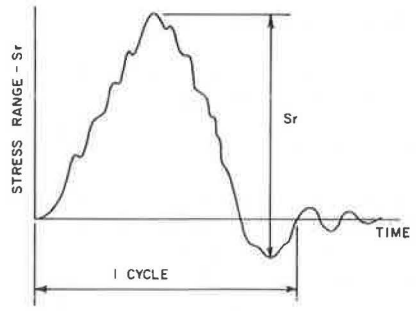

Figure 2. Stress-range histogram.

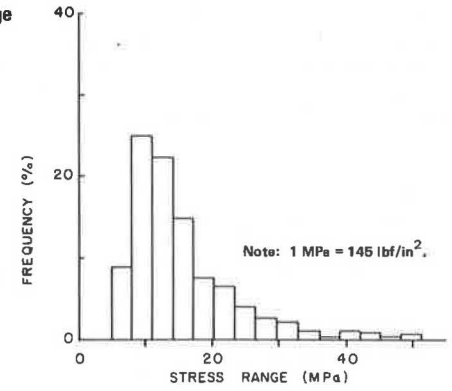

Figure 3. Simulated strain trace and associated counting levels.

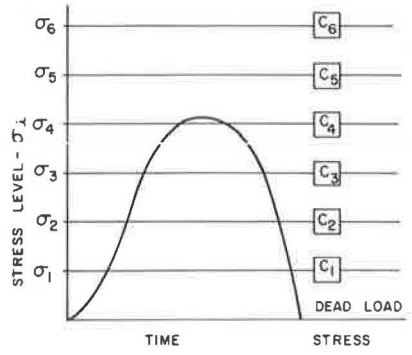

Figure 4. Simulated strain trace for actual loading cycle.

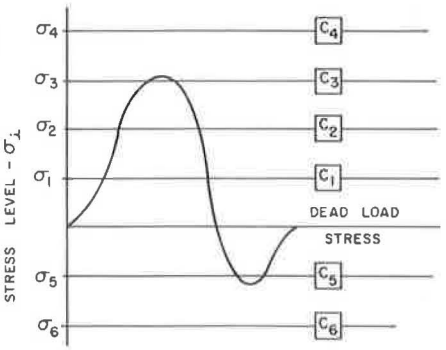

This procedure is initiated at the extreme positive and negative stress levels (in this case σ_5 and σ_8). By a process of elimination, the cumulative number of exceedences for each possible stress range is determined. The following example, which uses the stress levels and cumulative counter totals shown in Figure 5, illustrates the procedure.

First, the extreme counter totals (C_5) and (C_8) are compared. Because both C_5 and C_8 are zero, it is clear that there were no stress ranges in excess of σ_5 to σ_8. Next, counter totals C_4 and C_7 are compared. The lower total (C_4) is equal to the cumulative number of exceedences (Cr_6) of stress range (Sr_6) where Sr_6 is equal to the algebraic difference of σ_4 and σ_7. The higher value, in this case C_7, is retained and compared to the next descending counter (C_3). Because C_3 is less than C_6, $C_3 = Cr_5$ where Sr_5 is equal to the algebraic difference of σ_3 and σ_7. This procedure is continued until all counter totals have been considered.

Note that if C_3 had been equal to C_7 then $Cr_5 = C_3 = C_7$. In this case, no counter total is retained and the next comparison is made between C_2 and C_6. This procedure is followed whenever two counter totals are compared and found to be equal.

The final stress ranges and the cumulative number of exceedences for each range are also shown in Figure 5. The stress-range histogram for the data in Figure 5 is shown in Figure 6.

Cumulative Damage in Fatigue

In addition to determining the stress-range histogram, it may be desirable to estimate the long-range effects that fatigue has on the usable life of a bridge. Miner's cumulative damage theory (11) is commonly used as a basis for fatigue analysis and is used here, for simplicity, to show how data similar to those shown in Figure 6 may be used to determine the fatigue damage to a bridge caused by the random loading cycles encountered under service conditions. Damage is defined as the fractional part of the total life of the structure expended during any given number of cycles.

According to Miner's theory, the total damage is independent of the order of application of random loading cycles. Based on this assumption, the total damage is given by

$$\text{Damage} = \Sigma\,(n_i/N_i) < 1.0 \text{ (failure)} \qquad (3)$$

Figure 5. Determination of stress ranges.

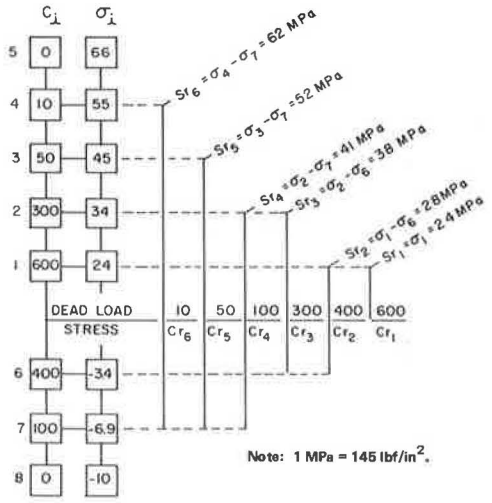

where n_ℓ is equal to the actual number of cycles at stress range (Sr_ℓ) and N_ℓ is equal to the number of cycles to failure at Sr_ℓ.

The number of cycles to failure (N) should be determined from a fatigue curve that is based on experimental data from structural details that are the same as, or similar to, the actual detail or details under consideration. A fatigue curve developed by Fisher and others for beams with end-welded cover plates (13) is shown in Figure 7.

Assume that n stress cycles with varying amplitudes (Sr) are applied to a bridge and that these cycles are then arranged in descending order of amplitude and plotted as shown in Figure 8, with the cycle number as ordinate and 1/N as abscissa. Damage done by the Kth cycle is equal to $1 \times (1/N_k)$, or the cross-hatched area shown in the figure. Thus the total damage done by the n cycles is

$$\text{Damage} = \sum_{i=1}^{n} 1 \times (1/N_i) \qquad (4)$$

which is clearly the total area under the curve. Furthermore, for any cycle (K), K - 1 is the number of cycles with amplitudes exceeding Sr_k. Thus, the curve shown in Figure 8 is also the cumulative exceedence curve, which can be closely approximated by plotting Cr_i versus $1/Nr_i$ as the number of cycles causing failure at a stress range of Sr_i. A sample damage curve is shown in Figure 9. The total damage may also be calculated numerically; such a calculation is given in the following table (1 MPa = 145 lbf/in^2):

Stress Range (MPa)	Exceedences	Damage Per Cycle ($1/N \times 10^8$)	Damage Total
76	0	105	
			[(105 + 58.8)/2] (10 - 0) = 819 x 10^{-8}
62	10	58.8	
			[(58.8 + 42)/2] (50 - 10) = 2016 x 10^{-8}
52	50	42	
			[(42 + 25.2)/2] (100 - 50) = 1680 x 10^{-8}
41	100	25.2	
			[(25.2 + 11.5)/2] (300 - 100) = 3670 x 10^{-8}
38	300	11.5	
			[(11.5 + 6.8)/2] (400 - 300) = 915 x 10^{-8}
28	400	6.8	
			[(6.8 + 3.4)/2] (600 - 400) = 1020 x 10^{-8}
24	600	3.4	

This procedure results in a figure for expended bridge life of 0.0101 percent.

INSTRUMENT DESIGN

Strain Transducer

The strain transducer is a sensing device used to produce an analog voltage signal proportional to the strain in a structural steel bridge girder. The sensing element used in this study is a Hewlett-Packard model 24DCDT-100, a direct-current differential transformer (DCDT) that requires 24-V excitation and provides an output signal of ±10 V over a displacement range of 0.24 cm (±0.1 in). The actual strain is therefore the displacement divided by the gauge length. The gauge length of the prototype transducer is 102 cm (40 in), which provides

Figure 6. Stress-range histogram and cumulative exceedence curve.

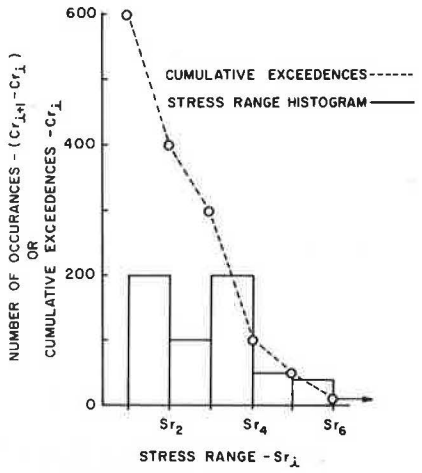

Figure 7. Fatigue curve for beams with end-welded cover plates.

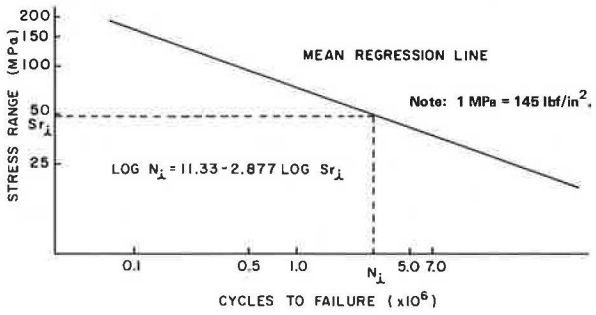

Figure 8. Cumulative fatigue damage.

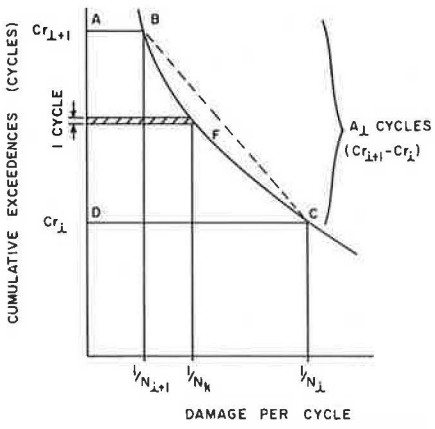

Figure 9. Sample damage curve.

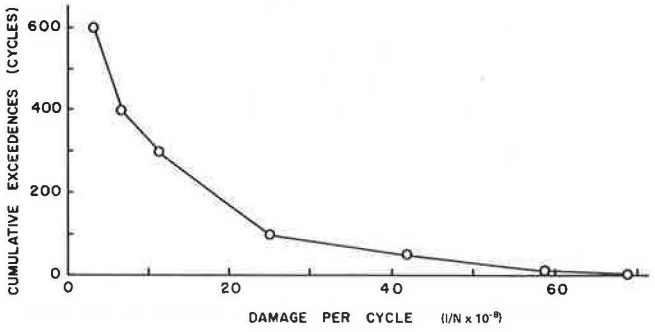

Figure 10. Prototype strain transducer.

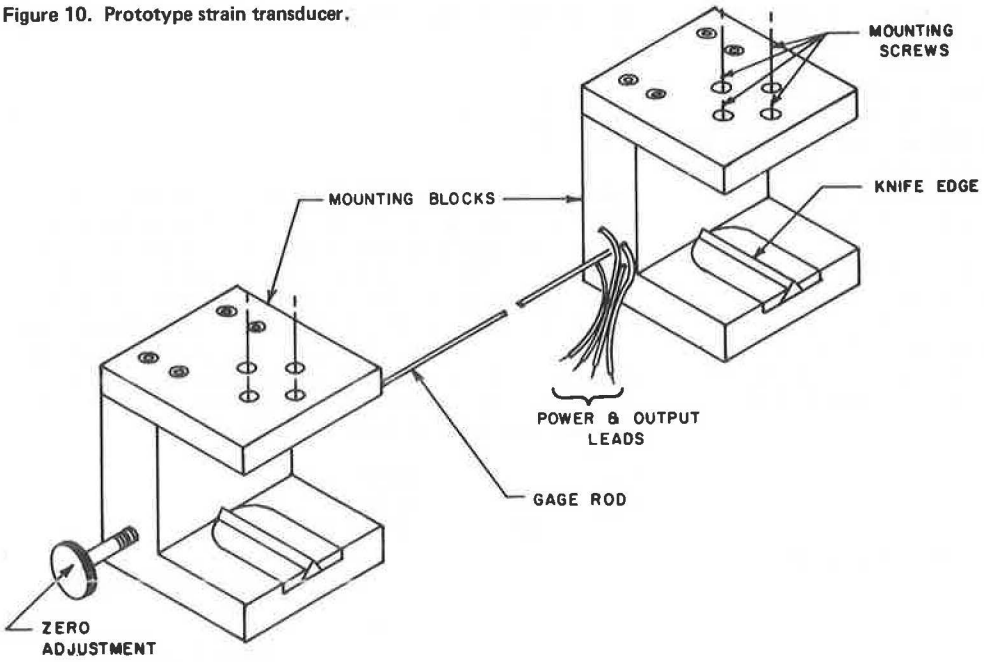

Figure 11. Cross-sectional view of prototype transducer.

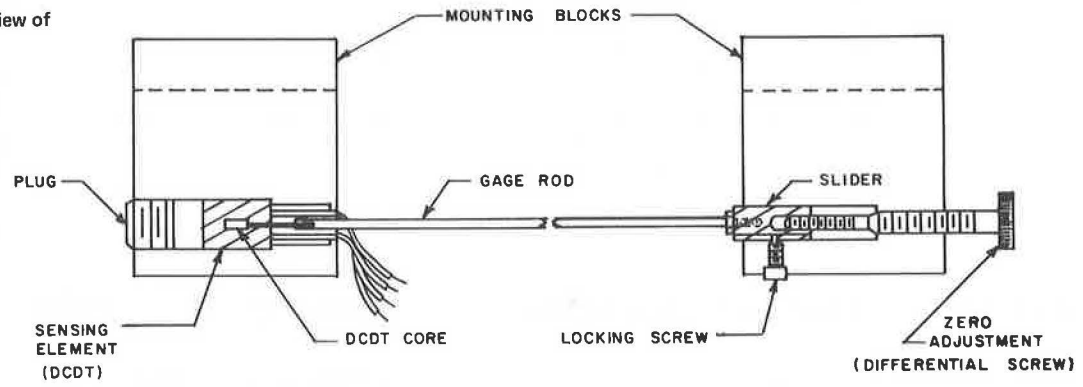

an output signal of approximately 4 mV/microstrain without amplification. The prototype transducer is shown in Figure 10; the DCDT is located internally in the mounting block on the right of the figure. A sectional view of the transducer and other internal parts is shown in Figure 11.

When the transducer is attached to a bridge girder, the gauge rod is supported at its midpoint by a teflon bearing mounted on a steel angle that clamps onto the bottom flange of the girder. This support minimizes vibration of the rod caused by wind and other dynamic loads and helps to conform the rod to the curvature of the girder.

A relatively small modification to the recorder would permit the use of an electric-resistance strain gauge as a transducer, greatly reducing the gauge length over which the strain is measured and cutting the power requirements in half. But one objective of this particular design was to produce a fairly rugged, reusable transducer that could be installed in the field without special tools or skill.

Recorder

The recorder is an electronic package designed to receive and monitor the output signal from the strain transducer. Inside the recorder, a series of ten counters, each triggered at a separately adjustable stress or strain level, record stress events as they occur. All counters are rearmed simultaneously when the input signal crosses the zero line. The recorder contains circuitry for filtering out base-line drift caused by temperature and other relatively long-term effects.

Power Supply

The instrument may be powered by any direct-current (dc) power source that satisfies the following requirements: 24-V system voltage (nominal); 38-mA strain transducer; 6-mA recorder. Because both the output of the strain transducer and the triggering voltages are directly proportional to the power-supply voltage, the instrument will function normally under dc power-supply fluctuations from 28 to 20 V.

The system has been tested with a power supply consisting of two 12-V automobile batteries rated at 342 kC (95 A·h). At 21°C (70°F) this battery pack will supply enough power for instrument operation up to approximately 80 d between recharges. Although this is an economical power supply that provides for long periods of operation, the size of the batteries requires a separate battery case. The 25-kg (55-lb) weight of each of these batteries also makes them rather difficult to handle in the field.

A pair of 12-V rechargeable dry cells intended for portable television sets has also been used to power the instrument. These batteries are much lighter and smaller and will fit inside the recorder cover. At 21°C (70°F) two of these batteries will power the unit for about 2 weeks between recharges. Commercial literature indicates that they can be recharged 30 or 40 times.

Total Instrument Package

The transducer, the recorder, and the power supply (except in the case where automobile batteries are used) all fit inside a tamper-proof 122 × 122 × 23-cm (48 × 48 × 9-in) enclosure. Both the transducer and the tamper-proof enclosure are clamped to the bottom flange of the steel girder with screws located inside the enclosure. No special preparation is required for the transducer.

Basic resolution of the electronic countercircuits is ±10 mV [0.52 MPa (75 lbf/in^2) of stress for steel], and the resolution is theoretically infinite. The calibration factor for the differential transformer varies 4 or 5 percent between transformers. The precision of the instrument is therefore dependent on the effort put into matching the recorder circuit to the transducer. However, a 1 or 2 percent match is not difficult.

Although a precise definition of the overall accuracy of the instrument would be quite complex, it is reasonable to assume that, for the majority of data collected on steel bridges, actual triggering levels will be within ±1.03 MPa (150 lbf/in^2) of the value set.

SUMMARY AND CONCLUSIONS

The self-monitoring instrument for load-history studies is presented here as an economical means for collecting data that reflect the actual service stresses occurring in a structural steel highway bridge. The availability of the instrument will make possible the collection of load-history data from a wider variety of bridges for much longer periods of time than may be obtained by using present techniques.

The complete system consists of (a) the strain transducer, (b) the recorder, and (c) the battery pack. System design is such that the instrumentation may be attached to a structural steel bridge girder and left in place for extended periods of time subject only to battery recharging at intervals of approximately 14 to 80 d, depending on the battery pack used. Simplified data-analysis techniques allow accumulated data to be used directly or in terms of bridge fatigue life. Installation of the instrument requires approximately 20 min, and batteries can be replaced and a set of readings taken in about 5 min. Field tests show that the instrument works well under field conditions.

ACKNOWLEDGMENT

The work reported here was conducted as a Highway Planning and Research study under the sponsorship of the Missouri State Highway Department in cooperation with the Federal Highway Administration, U.S. Department of Transportation. The opinions, findings, and conclusions expressed are not necessarily those of the Federal Highway Administration or the Missouri State Highway Department.

REFERENCES

1. D. G. Bowers. Loading History, Span #10, Yellow Mill Pond Bridge, I-95, Bridgeport, Connecticut. Connecticut Department of Transportation, HPR 175-332, Jan. 1973.
2. W. H. Munse, K. H. Lenzen, B. Yen, G. E. Nordmark, and J. Yao. Analysis and Interpretation of Fatigue Data. Journal of Structures Division, Proc., ASCE, Vol. 74, No. ST12, Paper 6283, Dec. 1968.
3. D. W. Goodpasture and E. G. Burdette. A Comparison of Bridge Stress History Results With Design Related Analyses. Univ. of Tennessee, Jan. 1973.
4. P. P. Christiano, L. E. Goodman, and C. N. Sun. Bridge Stress Range History. HRB, Highway Research Record 382, 1972, pp. 1-12.
5. T. R. Douglas. Fatigue Life of Bridges Under Repeated Highway Loading. HRB, Highway Research Record 382, 1972, pp. 13-20.
6. C. P. Heins and R. L. Khosa. Comparison Between Induced Girder Stresses and Corresponding Vehicle Weights. HRB, Highway Research Record 382, 1972, pp. 21-26.
7. W. T. McKeel, C. E. Maddox, Jr., H. L. Kinnier, and C. F. Galambos. Loading History of Two Highway Bridges in Virginia. HRB, Highway Research Record 382, 1972, pp. 27-37.
8. G. R. Cudney. Stress Histories of Highway Bridges. Journal of Structures Division, Proc., ASCE, Vol. 94, No. ST12, Paper 6289, Dec. 1968.
9. C. F. Galambos and W. L. Armstrong. Acquisition of Loading History Data on Highway Bridges. Public Roads, Vol. 35, No. 8, June 1969.
10. C. F. Galambos and C. P. Heins, Jr. Loading History of Highway Bridges: Comparisons of Stress-Range Histograms. HRB, Highway Research Record 354, 1971, pp. 1-12.
11. M. A. Miner. Cumulative Damage in Fatigue. Journal of Applied Mechanics, Vol. 12, No. 1, Sept. 1945.
12. W. H. Munse and J. E. Stallmeyer. Fatigue in Welded Beams and Girders. HRB, Bulletin 315, 1962.
13. J. W. Fisher, K. H. Frank, M. A. Hirt, and B. M. McNamee. Effect of Weldments on the Fatigue Strength of Steel Beams. NCHRP, Rept. 102, 1970.
14. Dynamic Studies of Bridges on the AASHO Road Test. HRB, Special Rept. 71, 1962.
15. W. H. Walker. Dynamic Stresses and Deflections in Highway Bridges. 16th Annual Structural Engineering Conference, Univ. of Kansas, Lawrence, April 1971, and 12th Annual Bridge Engineering Conference, Colorado State Univ., Fort Collins, April 1971.
16. J. W. Baldwin, Jr. Impact Study of a Steel I-Beam Highway Bridge. Univ. of Missouri—Columbia, Engineering Experiment Station Series, No. 58, 1964.

Publication of this paper sponsored by Committee on Dynamics and Field Testing of Bridges.